

# WIRELESS ENGINEER

Vol. XXVII

MAY 1950

No. 320

## An Electrostatic Field Problem

THE stretched elastic threads that are so often used as analogies when considering pictures of electric and magnetic fields are liable to be carried too far and to lead to false conclusions. In Fig. 1 a positively-charged sphere is situated at the centre of a large metal spherical shell. An equal and opposite charge will be induced on the inner surface of the shell and, if the charge is  $q$  e.s. units,  $4\pi q$  lines of force will radiate symmetrically from the positively-charged

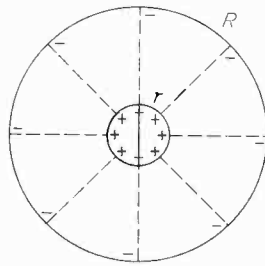


Fig. 1

sphere to the shell. The electric field will exert a radial force inwards on the shell and outwards on the small sphere, and anyone who has thoroughly absorbed the stretched elastic-thread analogy could be forgiven for jumping to the fairly obvious conclusion that the total force is the same on both. If the small sphere were split into two hemispheres each charged with  $+q/2$  they would mutually repel each other, but the stretched elastic thread analogy would probably lead to the obvious conclusion that the apparent repulsion was really due to the attractive forces of the stretched elastic threads, and that the mechanical reaction comes on the outer shell.

How wrong all this is can be seen at once by calculating the mechanical forces at the two surfaces. At any radius  $x$  the field strength  $\mathcal{E}$  (i.e., the number of lines per  $\text{cm}^2$ ) is equal to  $4\pi q/(4\pi x^2) = q/x^2$ . The mechanical tension is equal to  $\mathcal{E}^2/(8\pi)$ ; that is, to  $q^2/(8\pi x^4)$  per  $\text{cm}^2$ .

The total mechanical force over the spherical surface  $4\pi x^2$  is, therefore,  $q^2/(2x^2)$ , and falls off inversely as the square of the radius, although there is no change in the number of lines of force. If the radii of the inner and outer spheres are  $r$  and  $R$  respectively, the total forces over the two surfaces are  $q^2/(2r^2)$  and  $q^2/(2R^2)$  and if the inner charged sphere has a radius  $r$  of 1 cm and the outer shell a radius  $R$  of 1 metre, only a ten-thousandth part of the mechanical force on the small sphere is exerted on the whole surface of the outer shell. When the small sphere is divided into two parts, it follows that only a negligible part of the mechanical reaction involved in the repulsion of the two parts comes on the outer shell, and still less on the walls of the room if the outer shell is removed. Although the stretched elastic threads radiate from the small sphere, the stress in them falls off very rapidly, as if they were being gripped by myriads of invisible hands which take the stress.

The total radial force over a half the surface of the small sphere is  $q^2/(4r^2)$  and the resultant force tending to separate the two halves will be a half of this; viz.,  $q^2/(8r^2)$ . This is what the force would be between two point charges of  $q/2$  separated a distance of  $\sqrt{2}r$ . Similarly, the resultant force on half the large spherical shell will be  $q^2/(8R^2)$  which, as we have seen, is negligibly small. Where then must we look for the missing reaction  $q^2/(8r^2) - q^2/(8R^2)$ ? This is provided by the lateral pressure in the electric field. It is this lateral pressure that provides the myriads of invisible fingers which relieve the radial lines of the stress. The lateral pressure is also equal to  $\mathcal{E}^2/(8\pi)$  per  $\text{cm}^2$  and if we integrate this over the plane surface separating the two large hemispheres between the

radii  $r$  and  $R$  we get for the total repulsive force

$$\int_r^R \frac{Q^2}{8\pi} \cdot 2\pi x \cdot dx = \int_r^R \frac{q^2}{x^4} \cdot \frac{2\pi x}{8\pi} \cdot dx = \int_r^R \frac{q^2}{4x^3} \cdot dx$$

$$= \frac{q^2}{8} \left( \frac{1}{r^2} - \frac{1}{R^2} \right)$$

which for most practical purposes is equal to  $q^2/(8r^2)$ . The repulsive force in the field falls off very rapidly with increasing radius, so that about 90 per cent of the total repulsive force between the two charges is exerted by lateral pressure in the field within a radius of  $3r$ .

All the lines of force end normally on the spherical surface so that the ultimate force on the small hemispheres is a tension normal to the surface. At a short distance from the surface this radial tension is reduced and converted into a circumferential pressure, somewhat as shown in Fig. 2 in which the two dotted circles represent fictitious spherical shells which take up the tension of the small springs and convert it into

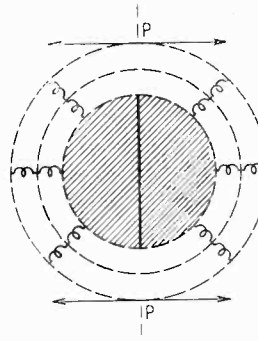


Fig. 2

The view that the apparent repulsion between two like charges placed close together is really due to attraction by the induced charges on the surrounding walls is thus quite wrong and due to a misconception of the nature of the forces in the electric field.

G. W. O. H.

## Oliver Heaviside

**T**HIS year is the centenary of the birth of Oliver Heaviside. He is now perhaps most widely known in connection with the E layer for, until quite recently, it was generally called the Kennelly-Heaviside layer. Kennelly in the U.S.A. and Heaviside in this country suggested at about the same time that such a layer might exist and that its presence would account for long-distance wireless propagation. In his article "Theory of Electric Telegraphy," which was written in June 1902 and published in the tenth edition of "Encyclopædia Britannica," Heaviside wrote "There may possibly be a sufficiently conducting layer in the upper air. If so, the waves will, so to speak, catch on to it more or less. Then the guidance will be by the sea on the one hand and the upper air on the other."

Probably his most important work, however, was in the development of operational methods of solving differential equations. Although his methods were not acceptable to many mathematicians of his day, they have stood the test of time and are now commonly used.

The Heaviside unit-impulse, or step-function, is famous and the analysis of the transient response of circuits is probably more often carried out by his basic methods than by any other. He originally developed them mainly for investigating the properties of cables which then formed the chief method of telegraph transmis-

sion. His theoretical analysis showed that for the distortionless transmission of a signal it was necessary properly to relate the capacitance, inductance, resistance and leakage of a cable, and that the natural inductance of a cable was much too small. He suggested, therefore, that the dielectric of the cable should be loaded with finely divided iron and later, he produced the alternative, and more practical, suggestion that the required increase of inductance should be obtained in lumps by means of inductance coils inserted in series with the cable at intervals.

This idea of loading a cable was too revolutionary for the times, 1893, and it was not for seven years that it was given a trial by Prof. M. I. Pupin at Columbia University. The results so confirmed Heaviside's theory that loading soon became normal practice and is still in common use.

Oliver Heaviside was born on 13th May 1850 at 55 King St., Camden Town and he died in Torquay on 4th February 1925. Wireless and electrical communication owe very much to him, how much is only now becoming widely realized. He was too much in advance of his generation for his work to be properly appreciated at the time. This appreciation, however, was not entirely withheld during his lifetime for, in his later years, he received some part of the honour due to him.

W. T. C.

# SECONDARY-EMISSION VALVE

*Wideband Amplifier for Decimeter Waves*

By G. Diemer and J. L. H. Jonker

(Philips Research Laboratories, Eindhoven, Netherlands)

**SUMMARY.**—An experimental secondary-emission valve is described. The high figure of merit ( $g_m/C = 3.0 \text{ mA/V-pF}$ ) that is obtained by adding one stage of secondary emission to an earthed-grid triode of rather conventional construction makes the valve useful as a wideband amplifier for those cases where a very low noise figure is not required; typical figures are: at 1 m wavelength 30 db gain ( $G$ ) with a bandwidth ( $B$ ) of 3.5 Mc/s, at 50 cm  $G = 15 \text{ db}$  with  $B = 20 \text{ Mc/s}$ , at 30 cm  $G = 10 \text{ db}$  with  $B = 10 \text{ Mc/s}$ . The maximum power output is for  $\lambda > 1 \text{ m}$  about 1.5 watts. At 7 m wavelength the noise figure amounts to 12 db; this rather high value is due to secondary emission. It is shown that for this secondary-emission noise a kind of space-charge smoothing effect exists.

It is well known that the high-frequency performance of wideband amplifiers is mainly governed by the ratio of the mutual conductance  $g_m$  to the valve capacitance  $C$  (provided that the ohmic losses are made as small as possible). In those cases where one is limited by the available cathode emission rather than by the static anode dissipation, it is possible to increase both the mutual conductance and the anode current by a factor  $\delta$  by adding one stage of secondary emission (in practical cases  $\delta$  may amount to about 5)<sup>1</sup>. With careful design the capacitance need not be increased by this. In those cases where the static anode dissipation of the normal valve is already a maximum, it is better to keep the anode current unchanged when adding the secondary-emission stage, thus decreasing the cathode current  $I_k$  by a factor  $\delta$ , which results in a considerable decrease of input damping and an increase of  $g_m/I_k$ . In this article it will be shown that high values of  $g_m/C$  and  $g_m/I_k$  can be obtained in such a secondary-emission valve, even when the cathode-grid construction is rather conventional (no small distances; mounted on mica).

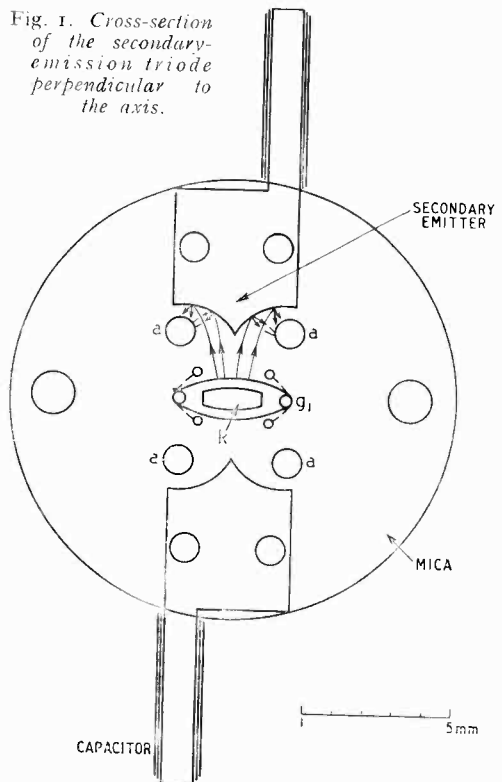
Wagner and Ferris<sup>2</sup> have already described a secondary-emission valve operating at  $\lambda = 60 \text{ cm}$ . Though the valve described here is of a simpler electrode construction, which is possible because of the good life obtained with a caesium-oxide emitter<sup>3</sup>, it operates up to frequencies of 1000 Mc/s ( $\lambda = 30 \text{ cm}$ ). A drawback of the secondary-emission valve is its relatively high noise figure. As is well known the random fluctuations of  $\delta$  introduce an additional noise.<sup>4</sup> Noise measurements on the new u.h.f. secondary-emission valve have been published by Van der Ziel and Versnel<sup>5</sup>; the minimum noise figure is 12 db.

## 1. Construction and Static Data

Figs. 1 and 2 give cross-sections of the valve, and the following points are of particular interest.

(a) The valve is of cheap and simple construction; it is an earthed-grid triode in which the electrodes are mounted on mica. The grid wires have a diameter of  $35 \mu$ ; the distance  $d_{kg}$  between the cathode surface and the centre of the grid wires is  $120 \mu$ .

Fig. 1. Cross-section of the secondary-emission triode perpendicular to the axis.



(b) Ohmic losses are reduced by connecting several molybdenum pins in parallel and using broad copper-plated connectors within the valve.

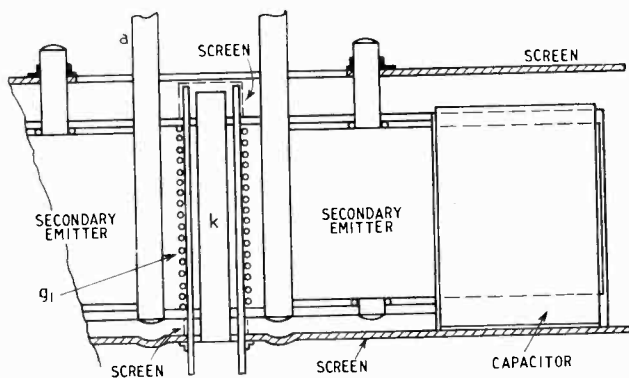
(c) A small value of the valve capacitance is obtained by using a special electrode con-

MS accepted by the Editor, September 1949

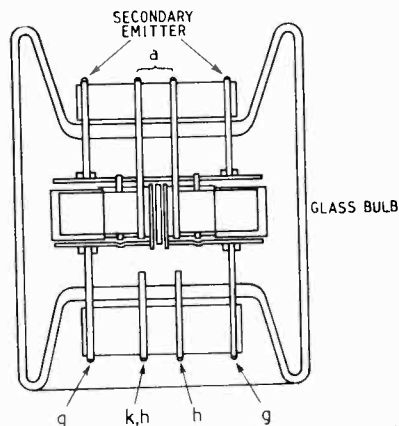
struction, developed with the help of large scale models on a rubber sheet<sup>6</sup>; the primary beams are focused by small focusing rods on a V-shaped secondary emitter. The anode (from which the output signal has to be taken) consists of four 1-mm molybdenum rods, directly sealed through the powdered-glass bottom; in this way both the r.f. and heat conductivity are good.

emission as well as of the life is obtained for caesium oxide on copper, by making the temperature of the secondary emitter as low as possible. This low temperature results from the 'open' electrode construction: the secondary emitter is heated very little by radiation from the anode and cathode. The secondary emitter is provided with cooling fins.

(g) The electron optics for the primary and the



(a)

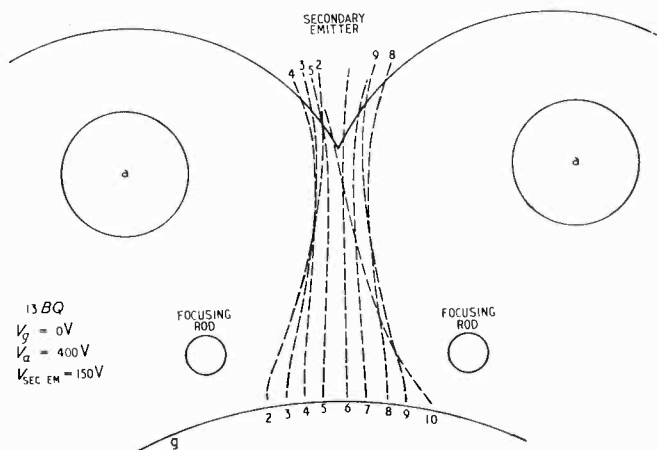


(b)

Fig. 2 (above). (a) Electrode construction on a larger scale.

(b) Cross-section of the valve through the axis of the cathode.

Fig. 3 (right). Electron trajectories drawn from a photograph from a large-scale model of the valve on a rubber sheet;  $V_{g1} = 0$  V;  $V_{sec.em.} = 150$  V;  $V_a = 400$  V.



(d) The spread in transit time should be as small as possible. For this reason, as well as for the reason (a) mentioned above, only one stage of secondary emission is used. Fig. 3 gives a drawing according to a photograph taken from rubber-sheet experiments. From such photographs an estimate of the spread in transit-time can be made (see below).

(e) Feedback from the anode to the cathode is made very small by the earthed-grid construction with good internal shielding, while the secondary emitter is connected to the internal grid shield by a built-in capacitor, the cooling fin being one of the capacitor electrodes. The valve is 'double-ended,' the leads of the secondary emitter and of the grid consist of a ring of pins connected in parallel and adapted for coaxial input and output circuits.

(f) A high value of the coefficient of secondary

secondary electrons should be such that for a large range of voltages at the secondary emitter and at the anode both the trajectories of the primaries and of the secondaries are 'good'; that is to say, (1) for a high value of  $V_a$  no primaries should be lost by going directly to the anode and (2) for low values of  $V_a - V_{sec.em.}$  the field strength at the secondary emitter should remain everywhere such that all secondaries are drawn away.

These two conditions are more or less contradictory when using an electrode arrangement

like that of Fig. 1. The effective value of  $\delta = I_a/I_k$ , (where  $I_k$  is the cathode current and  $I_a$  the anode current) was measured as a function of  $V_a - V_{sec.em.}$  for a series of valves having different electrode spacings; the voltage of the secondary emitter was constant ( $V_{sec.em.} = 150$  V).

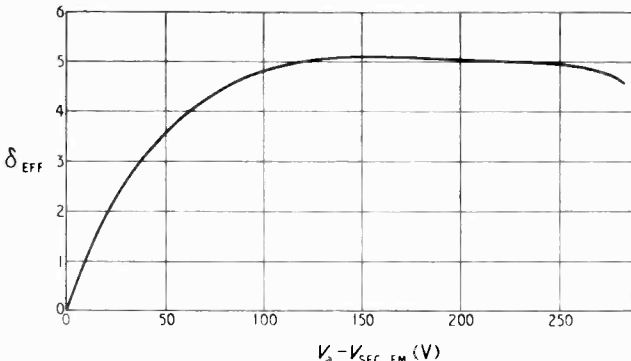
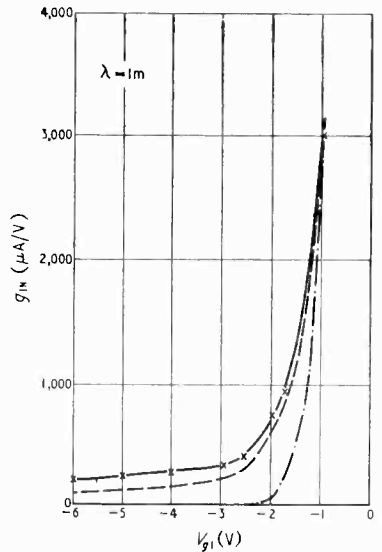


Fig. 4 (above). Effective value  $\delta_{eff} = I_a/I_k$  of the coefficient of secondary emission versus voltage difference between anode and secondary emitter.  $V_{sec.em.} = 150$  V;  $I_a = 10$  mA.  $I_k =$  total cathode current.

Fig. 5 (right). Input conductance  $g_{inp}$  of the secondary-emission triode at  $\lambda = 1$  m as a function of control grid voltage  $V_{g1}$ .  $V_a = 300$  V;  $V_{sec.em.} = 150$  V. — Total conductance at  $\lambda = 1$  m; ——— electronic conductance; - - - - - static value of the input slope  $g_{mi} = dI_k/dV_g$ .



In Fig. 4 a curve is given for the valve that proved to be the best compromise: for a large range of  $V_a$ -values  $\delta$  has nearly the maximum value.

In Table 1 different static values of the valve characteristics are given.

Attention may be drawn to the high value of the amplification factor  $\mu$  (400) which in earthed-grid amplifiers is important for a high energy gain (see K. S. Knol and A. van der Ziel)<sup>7</sup>. From the electrode arrangement shown in Fig. 1 it may be seen that, indeed, the anode rods have a very small 'Durchgriff' through the control grid.

TABLE 1

Control-grid voltage (volts) .. .. .	1.1
Anode current (mA) .. .. .	18
Anode voltage (volts) .. .. .	350
Sec. em. voltage (volts) .. .. .	150
Coeff. of sec. em. $\delta_{eff} = I_a/I_k$ .. .. .	4.5
Mutual conductance $g_m = \frac{dI_a}{dV_g}$ (mA/V) .. .. .	24
Maximum anode dissipation (watts) .. .. .	6
Amplification factor $\mu$ .. .. .	400
Valve capacitance $C_{gk}$ (pF) .. .. .	4.6
$C_{av}$ (pF) .. .. .	3.3
$C_{ak}$ (pF) .. .. .	0.018
Band merit $\frac{g_m}{C_{av} + C_{gk}} \left( \frac{\text{mA}}{\text{V} \cdot \text{pF}} \right)$ .. .. .	3.0

## 2. U.h.f. Properties of the Valve

### 2.1 Input and output conductance

The input and output conductance of the valve were measured at 1 m wavelength ( $f = 300$  Mc/s) by means of a coaxial Lecher wire. The method of measurement was the same as

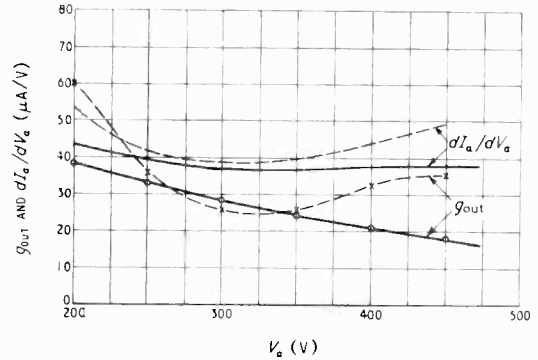


Fig. 6. Electronic output conductance  $g_{out}$  of the secondary-emission triode as a function of anode voltage  $V_a$  (full drawn line) and static value of the output conductance  $g_o = dI_a/dV_a$  (dotted line).

described by Van Hofweegen<sup>8</sup>. Figs. 5 and 6 give these conductances as a function of control-grid voltage and anode voltage respectively. From these figures the u.h.f. values of the electronic conductances may be compared with the corresponding static value. For normal operating voltages ( $V_a \approx 300$  V) the u.h.f. electronic output conductance is smaller than the corresponding static value, as might be expected from the phase angle of the mutual conductance due to transit-time effects (see also Section 2.2). The relatively large input damping at large negative values of  $V_{g1}$  which varies nearly as  $|V_{g1}|^{-2}$

must be explained as total-emission damping caused by electrons that return in front of the potential minimum (see also G. Diemer and K. S. Knol<sup>9,10</sup>).

Together with the measurements of the conductance the corresponding valve lead inductance could be determined. In Table 2 a survey of the results is given, including the resonance wavelength of the short-circuited input and output leads.

TABLE 2

Lead inductances and total valve conductances at  $\lambda = 1 \text{ m}$ .

	cold valve	warm valve	
		$V_{g1} = -6 \text{ V}$ $I_a = 0 \text{ mA}$	$V_{g1} = -1.4 \text{ V}$ $I_a = 12 \text{ mA}$
Input conductance ( $\mu\text{A/V}$ ) ..	60	200	$\sim 3000$
Output conductance ( $\mu\text{A/V}$ ) ..	20	20	55
		input	output
Lead inductance ( $10^{-8}\text{H}$ ) ..		0.9	0.8
$\lambda_{res}$ (cm) ..		40	30

As may be seen from the conductances of the cold valve, the ohmic losses are small; this is important for a high energy gain (see Van der Ziel<sup>11</sup>).

The small values of the lead inductances together with the small valve capacitances result in a high resonant frequency of the short-circuited valve.

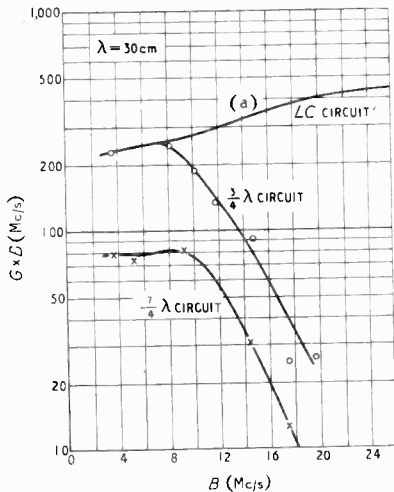


Fig. 7. Bandmerit  $G \times B$  versus bandwidth  $B$  for two different lengths of the Lecher-wire circuits at  $\lambda = 30 \text{ cm}$ ;  $V_{sec.em.} = 130 \text{ V}$ ;  $V_a = 420 \text{ V}$ ;  $V_{g1} = -0.5 \text{ V}$ . Curve (a): theoretical curve for an LC-circuit.

## 2.2 Bandwidth and gain at wavelengths below 1 m.

These measurements were performed by means of the matching transformers of Van Hofweegen and Knol<sup>12</sup> in the well-known way. The bandwidth is here defined as being the width between the 3-db points. Care was taken that the coaxial connections between the valve and the transformers were made as small as possible in

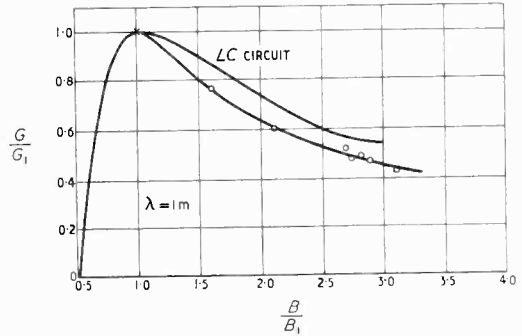


Fig. 8. Gain  $G$  versus bandwidth  $B$  at  $\lambda = 1 \text{ m}$ ;  $G$  and  $B$  are varied by mismatching.  $G_1 = \text{optimum gain}$ ,  $B_1 = \text{bandwidth at optimum gain}$ .

order to avoid a decrease of bandwidth. Nevertheless, in most of the measurements the bandwidth  $B$  was smaller than could have been obtained by an LC-circuit, as may also be seen from Fig. 7 where the bandmerit  $G \times B$  is plotted versus  $B$ , both for the Lecher wires (experimental) and for an LC-circuit (theoretical) for the case where feedback can be neglected. In our case the feedback due to the internal resistance of the valve is, indeed, very small because of the high value of the amplification factor. The bandwidth was varied by mismatching the output. At  $\lambda = 1 \text{ m}$ , where we could work with a  $\lambda/4$  Lecher wire, the discrepancies were much smaller (see Fig. 8). Probably part of the discrepancies must be ascribed to the influence of feedback capacitance between anode and cathode.

Fig. 9 shows  $G$  and  $B$  as a function of anode voltage. The full-drawn line refers to a different type of experimental valve, which had a greater distance between the anode and the secondary emitter. In Fig. 10  $G$  and  $B$  are shown as a function of frequency for the same valves as in Fig. 9. The gain decreases greatly with increasing frequency, especially for the valve with the larger electrode distances. With a higher anode voltage the decrease is smaller. From this we conclude that, especially at the upper frequency limit, transit-time effects have a large influence. We tried to predict this decrease of gain by computing the input and output damping and the mutual conductance according to the well-known methods of transit-time theory (see,

e.g., Bakker and De Vries<sup>13</sup>) including the influence of spread in transit time of the primaries and the secondaries (see Malter<sup>14</sup>) and of ohmic losses in the electrode leads, the latter by extrapolating from the values measured at 300 Mc/s according to a 5/2-power law. In doing so, it was shown, that at 1 m wavelength both the bandwidth and the gain agreed rather well with the calculated values, but the decrease of gain at higher frequencies was much faster and the increase of bandwidth smaller than might be expected from the two effects mentioned above. Possible causes for this are:—

(a) the influence of feedback by the capacitance between the anode and the cathode, which in the neighbourhood of 1000 Mc/s can no longer be neglected (see also Van der Ziel and Knol<sup>15</sup>; the formulae given by the latter authors are, however, difficult to apply in our case because our electrode arrangement is rather complicated);

(b) the influence of space charge, which in the rubber-sheet experiments could not be taken into account, but which may result in a larger spread in transit time than is predicted by models of the electron trajectories as shown on the rubber sheet.

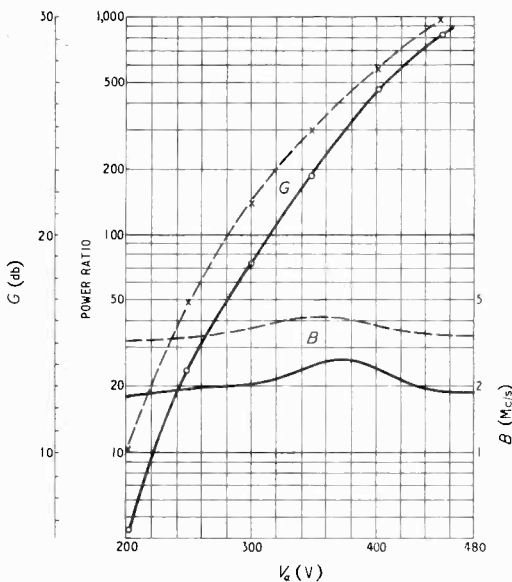


Fig. 9. *G* and *B* as a function of anode voltage  $V_a$  with  $\lambda = 1$  m.  $V_{sec-em.} = 150$  V;  $V_{o1} = -0.5$  V. The dotted curves are for a normal valve similar to that of Fig. 1 and the full-line curves for a valve with greater spacing between the output electrodes.

### 2.3 Power output v. frequency.

The secondary-emission valve has a lower efficiency than a pentode or a beam tetrode, because

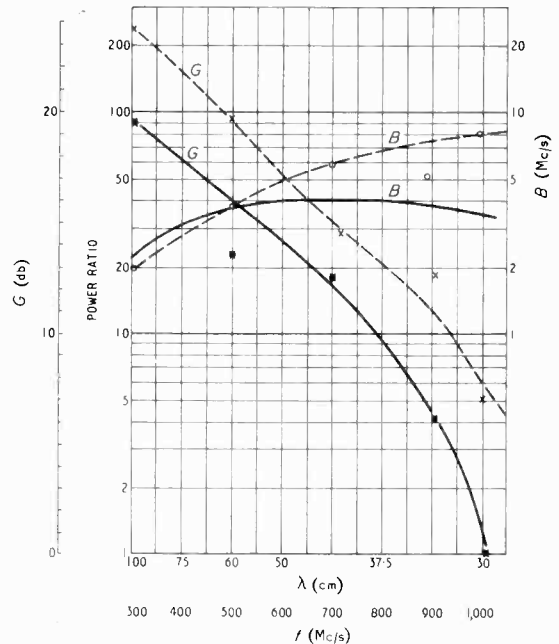


Fig. 10. *G* and *B* as a function of frequency for the values referred to in Fig. 9.  $V_{o1} = -0.7$  V.

a certain amount of energy is lost as constant heat dissipation of the secondary emitter and the  $I_a - V_a$  characteristic has not such a sharp knee as have other valves (this may be seen from the  $\delta$ -curve given in Fig. 4).

From the static characteristics for long wavelengths a maximum efficiency of about 30% may be estimated.

In Fig. 11 the efficiency  $\eta$  is plotted against  $\lambda$ . We see that, for  $\lambda > 1$  m,  $\eta \approx 30\%$ . Near the short-wave limit ( $\lambda \approx 30$  cm) the efficiency decreases rapidly due to the same causes that decrease the gain. In the same illustration curves are given for the driving power  $P_i$  and the output power  $P_o$ .

### 2.4 Noise measurements.

For the calculations and some of the measurements on the noise of this valve we refer to Van der Ziel and Versnel<sup>15</sup>, the following formula for the noise figure  $F$  can be derived from their article:

$$F - 1 = \alpha = \frac{\epsilon R_e + \frac{K - \delta}{\delta} \cdot \frac{e}{2kT} I_k (R_e + R_a)^2}{R_a} \quad \dots \quad (1)$$

in which  $R_e$  = electronic input resistance

$\epsilon = \frac{R_n}{R_e}$ ,  $R_n$  being the noise resistance due to shot noise

$e$  = electronic charge

$k$  = Boltzmann's constant

$T$  = room temperature ( $^{\circ}K$ )

$\delta$  = coefficient of secondary emission =

$$\frac{I_a}{I_c} = \sum_m \beta_m m; K = \frac{I}{\delta} \sum_m \beta_m m^2,$$

$\beta_m$  being the probability of the emission of  $m$  secondaries due to one single primary electron.

Formula (1) is valid under the following assumptions:

- (a) the conductances are purely electronic
- (b) partition noise of the primaries is negligible
- (c) no space charge between the anode and the secondary emitter.

The measurements reported by Van der Ziel and Versnel at  $\lambda = 7$  m agreed rather well with Equ. (1), giving a minimum noise figure  $F = 16$  ( $\approx 12$  db) at a suitably chosen value of the aerial resistance  $R' = 500 \Omega$ . (See Fig. 12.)

In order to investigate whether the influence of the space charge between secondary emitter and anode might result in a noise suppression of the secondary-emission noise, similar to the well-known cushion effect of the space-charge-limited primary emission, some additional noise measurements were performed for a large range of anode and secondary-emission voltages\*. At small values of  $V_a - V_{sec.em.}$  we found the experimental values to be smaller than the theoretical. In this case there is a large space

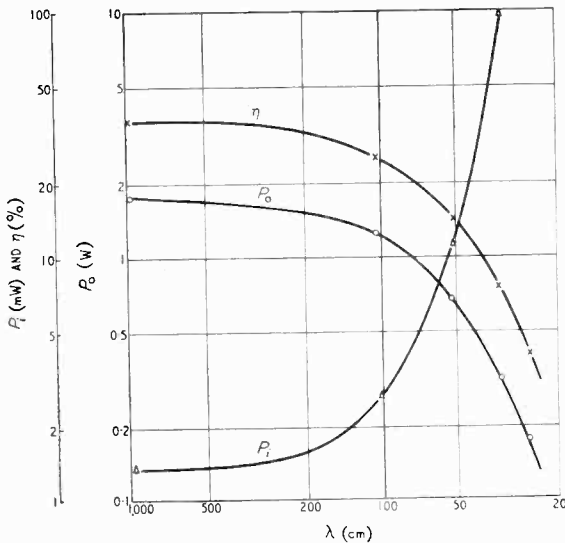


Fig. 11. Output power  $P_o$ , input power  $P_i$  and efficiency  $\eta$  as a function of frequency.

charge near the secondary emitter. Because, especially, the high momentary values of  $\delta$

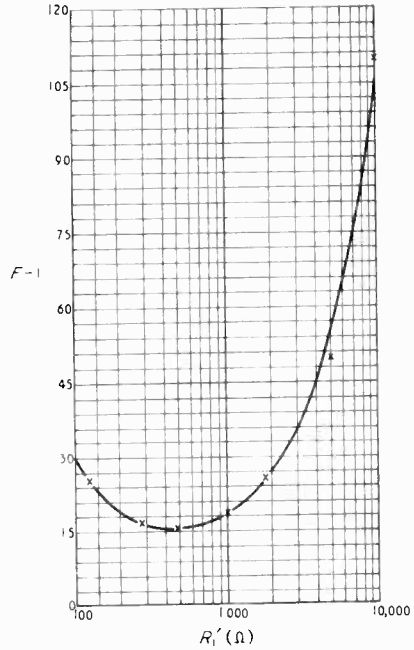


Fig. 12. Noise of the secondary-emission valve at  $\lambda = 7$  m.  $\alpha = F - 1$  as a function of aerial resistance  $R_1$  according to Van der Ziel and Versnel<sup>4</sup>.

contribute to  $K$  (and so to the noise) and because these large amounts of secondaries per single primary electron will be correlated to small initial velocities of the secondaries, one must expect that these large momentary values of  $\delta$  will be more or less suppressed by space charge in front of the secondary emitter. We think this effect to be the cause of the phenomenon mentioned above. The effect is, however, not large enough to reduce the secondary-emission noise to a value that would be of the same order of magnitude as the primary shot-effect noise.

According to Van der Ziel<sup>5</sup> lower noise figures may be obtained by working with a still higher value of  $g_m/I_c$ ; this could be done with smaller distances between cathode and control grid, but it introduces a more complicated valve construction.

### 3. Conclusions

It is possible to arrive at very high figures of merit for a triode of rather simple construction, by introducing one stage of secondary emission. This makes wideband amplification up to bandwidths of more than 20 Mc/s possible at decimeter waves. Because of its relatively high noise figure the valve is especially useful for those purposes where minimum noise figures are not required (last stages of i.f. amplifiers, power amplifiers).

\* These measurements were performed with the collaboration of Dr. K. S. Knol and Mr. A. Versnel.

## REFERENCES

- <sup>1</sup> J. L. H. Jonker and A. J. W. M. van Overbeek, *Wireless Engr.*, Vol. 15, pp. 150-156, 1938.
- <sup>2</sup> H. M. Wagner and W. R. Ferris, *Proc. Inst. Radio Engrs*, Vol. 29, pp. 598-602, 1941.
- <sup>3</sup> M. Chauvierre, *Tele-Tech*, Vol. 6, No. 7; pp. 69, 98, 105; 1947.
- <sup>4</sup> M. Ziegler, *Physica*, The Hague, Vol. 2, pp. 415-416, 1935.
- <sup>5</sup> A. van der Ziel and A. Versnel, *Philips Res. Rep.*, Vol. 3, pp. 255-270, 1948.
- <sup>6</sup> P. H. J. A. Kleynen, *Philips tech. Rev.* Vol. 2, pp. 338-345, 1937.
- <sup>7</sup> A. van der Ziel and K. S. Knol, *Philips Res. Rep.*, Vol. 4, pp. 168-178, 1949.
- <sup>8</sup> J. M. van Hoiveegen, *Philips tech. Rev.*, Vol. 8, pp. 16-24, 1946.
- <sup>9</sup> G. Diemer and K. S. Knol, *Physica*, The Hague, Vol. 15, pp. 459-462, 1949.
- <sup>10</sup> G. Diemer and K. S. Knol, *Philips Res. Rep.*, Vol. 4, pp. 321-333, 1949.
- <sup>11</sup> A. van der Ziel, *Philips Res. Rep.*, Vol. 1, pp. 381-399, 1946.
- <sup>12</sup> J. M. van Hoiveegen and K. S. Knol, *Philips Res. Rep.*, Vol. 3, pp. 140-155, 1948.
- <sup>13</sup> C. J. Bakker and G. de Vries, *Physica*, The Hague, Vol. 2, pp. 683-697, 1935.
- <sup>14</sup> L. Malter, *Proc. Inst. Radio Engrs*, Vol. 29, pp. 587-598, 1941.

# PHASE DISTORTION IN FEEDERS

## *Effect of Mismatching on Long Lines*

By L. Lewin,\* J. J. Muller, and R. Basard†

(\*Standard Telecommunication Laboratories Ltd., London, and †Matériel Téléphonique, Paris)

### 1. Introduction

IT is well known that variations of delay time with frequency for any unit of a radio system can cause a distortion of the signal. A mismatch at the end of a long feeder is one such source of variable delay, and an investigation of its effects has been initiated by Friis.<sup>1</sup> He finds the phase delay for a constant frequency input as a function of that frequency, but the results are not immediately applicable to frequency-modulated signals, and it is necessary to apply the variable-frequency analysis of Carson and Fry and others<sup>2</sup>. When this is done, a serious limitation of the method becomes apparent: with feeder lines of any appreciable length, the phase changes so rapidly with frequency that the first few terms of the expansion are insufficient, with the result that for a complete result the work becomes very clumsy and laborious. A fresh approach therefore seems desirable. This is provided by considering the system to support a series of running waves of various instantaneous frequencies, and reflected within the confines of the feeder, rather than the constant-frequency standing-wave formulation used by Friis.

### 2. Production of Waves in the Feeder

Let us consider an injected signal of carrier frequency  $f_c$  frequency modulated by a single tone video signal  $\Delta f \cdot \sin(2\pi f_a t)$  where  $\Delta f$  and  $f_a$  are respectively the peak frequency deviation and the modulating frequency. We write  $\omega_c = 2\pi f_c$ ,  $\Delta\omega = 2\pi\Delta f$  and  $\omega_a = 2\pi f_a$ , so that the modulated carrier can be written as

$$\cos [f(\omega_c + \Delta\omega \sin \omega_a t)dt] = \cos [\omega_c t + s(t)]$$

where  $s(t) = -(\Delta\omega/\omega_a) \cos \omega_a t$

If the signal is sent along a line of length  $l$ , a portion of the wave, depending on the mismatch at the far end, is reflected, and returns towards the transmitter. If the latter is also mis-matched, a portion of the reflected wave is sent out along the line again, and supplements the wave actually being transmitted at the time, and which is of a slightly different frequency, since the wave is frequency modulated. The wave leaving the feeder at any instant is accordingly a composite one, being composed of waves generated at different times, but delayed by reflections within the feeder. There will, of course, be multiple reflections, but if the mismatches are small, the dominant interference comes from that wave which has been reflected but once from each end of the feeder before leaving it.

If we introduce the time delay  $\tau$  along the feeder, and the group velocity,  $v$ , of the waves, then  $\tau = l/v$  and we find for the transmitted signal,  $S(t)$

$$S(t) = \cos [\omega_c t + s(t)] + r_1 r_2 e^{-2\alpha l} \cos [\omega_c(t - 2\tau) + s(t - 2\tau) + \theta_1 + \theta_2] \dots \quad (1)$$

Here,  $r_1$ ,  $r_2$  and  $\theta_1$ ,  $\theta_2$  are respectively the reflection coefficients and phase changes occurring at each end of the feeder, whilst  $\alpha$  is the attenuation constant for the line. Unless  $\tau$  is such that  $s(t - 2\tau) = s(t)$  (a case treated later), the two terms of equation (1) will be of different frequencies, so that the composite signal will involve  $s(t)$  in a non-linear way, with consequent distortion.

### 3. Production of Phase Distortion

At reception, we assume that the wave is first amplitude limited, and then put through the discriminator networks, which produce an output proportional to the instantaneous frequency of the signal  $S(t)$ . Now equation (1) can be put in the form

$$S(t) = A \cos [\omega_c t + s(t)] + B \sin [\omega_c t + s(t)]$$

where

$$A = 1 + r_1 r_2 e^{-2\alpha l} \cos [2\omega_c \tau + s(t) - s(t - 2\tau) - \theta_1 - \theta_2] \dots \dots \dots (2)$$

and

$$B = r_1 r_2 e^{-2\alpha l} \sin [2\omega_c \tau + s(t) - s(t - 2\tau) - \theta_1 - \theta_2]$$

This follows by putting  $\omega_c(t - 2\tau) + s(t - 2\tau) + \theta_1 + \theta_2 = [\omega_c t + s(t)] - [2\omega_c \tau + s(t) - s(t - 2\tau) - \theta_1 - \theta_2]$  in the second term of equation (1) and expanding.

Equation (2) can be re-written  $S(t) = \sqrt{A^2 + B^2} \cos [\omega_c t + s(t) - \phi]$  where  $\tan \phi = B/A$ . The amplitude limiting removes the factor  $\sqrt{A^2 + B^2}$  so that  $\phi$  represents the phase distortion due to the mis-matches. Since  $B \ll r_1 r_2 e^{-2\alpha l}$ , which is assumed small, and  $A \approx 1$ ,  $\phi$  will be small. This gives the approximation  $\phi \approx B$ .

Now the output of the discriminator networks is proportional to the instantaneous frequency of the amplitude-limited signal, and hence to  $\omega_c + s'(t) - d\phi/dt$ . Of this,  $\omega_c$  can be ignored while  $s'(t) = \Delta\omega \sin(\omega_a t)$  represents the recovered signal. The last term contains the distortion. Carrying out the differentiation we get an output

$$\Delta\omega \cdot \sin(\omega_a t) - d/dt \{r_1 r_2 e^{-2\alpha l} \sin [2\omega_c \tau + s(t) - s(t - 2\tau) - \theta_1 - \theta_2]\} (3)$$

Now  $s(t) - s(t - 2\tau) = 2\Delta\omega\tau$ .

$$\sin\{\omega_a(t - \tau)\} \sin(\omega_a\tau)/\omega_a\tau$$

The quantity  $2\Delta\omega\tau \cdot \sin(\omega_a\tau)/\omega_a\tau$  which occurs frequently will be denoted by  $y$ . Expanding formula (3) we get for the output

$$\Delta\omega \sin(\omega_a t) - r_1 r_2 e^{-2\alpha l} \sin(2\tau\omega_c - \theta_1 - \theta_2) d/dt [\cos [y \sin\{\omega_a(t - \tau)\}]] + r_1 r_2 e^{-2\alpha l} \cos(2\tau\omega_c - \theta_1 - \theta_2) d/dt [\sin [y \sin\{\omega_a(t - \tau)\}]] \dots \dots \dots (4)$$

### 4. Harmonic Production

If we use in (4) the Fourier-Bessel expansion of  $\sin[y \sin\{\omega_a(t - \tau)\}]$  and  $\cos[y \sin\{\omega_a(t - \tau)\}]$ , we can find the various harmonics produced. Ignoring the small amount of recovered signal that appears from the distortion terms, we find

Recovered Signal

$$\Delta\omega [\sin(\omega_a t)]$$

Second Harmonic

$$2r_1 r_2 e^{-2\alpha l} (2\omega_a) J_2(y) \sin(\theta) [\sin\{2\omega_a(t - \tau)\}]$$

Third Harmonic

$$2r_1 r_2 e^{-2\alpha l} (3\omega_a) J_3(y) \sin\left(\theta + \frac{\pi}{2}\right) [\cos\{3\omega_a(t - \tau)\}]$$

Fourth Harmonic

$$2r_1 r_2 e^{-2\alpha l} (4\omega_a) J_4(y) \sin(\theta + \pi) [\sin\{4\omega_a(t - \tau)\}] \dots \dots \dots (5)$$

where  $\theta = 2\tau\omega_c - \theta_1 - \theta_2$

In this equation, the last factor in square brackets is the form of the harmonic, and the rest of the expression is its amplitude.  $J_2(y)$ ,  $J_3(y)$ , etc., are Bessel functions, and are tabulated in, for example "Tables of Functions," p. 156 *et seq.* by Jahnke-Emde. All the harmonics are delayed by an amount  $\tau$  with respect to the fundamental. The terms  $\sin(\theta + n\pi/2)$  are normally indeterminate. They depend not only on the unknown phase changes  $\theta_1$  and  $\theta_2$ , but also on the precise electrical length of the feeder and the radio frequency. In a multi-repeater system, such terms would appear randomly phased, and hence would add up 'power-wise' from repeater to repeater. It is convenient, therefore, to give them their r.m.s. values of  $1/\sqrt{2}$ . But it should always be borne in mind that for any one particular set-up these terms will be quite definite, and can be, for example, zero for certain frequencies or lengths of feeder.

Accordingly we find

$$\frac{2nd \text{ Harmonic}}{\text{Fundamental}} = \sqrt{2} r_1 r_2 e^{-2\alpha l} (2\omega_a/\Delta\omega) J_2(y)$$

$$\frac{3rd \text{ Harmonic}}{\text{Fundamental}} = \sqrt{2} r_1 r_2 e^{-2\alpha l} (3\omega_a/\Delta\omega) \cdot J_3(y) (6)$$

$$\frac{nth \text{ Harmonic}}{\text{Fundamental}} = \sqrt{2} r_1 r_2 e^{-2\alpha l} (n\omega_a/\Delta\omega) J_n(y)$$

$$\text{where } y = 2\Delta\omega\tau \cdot \sin(\omega_a\tau)/\omega_a\tau$$

To get the harmonic margins in decibels we simply take  $20 \log_{10}$  of the above expressions.

It is clear from equation (6) that the margins of the harmonics with respect to the fundamental depend on the modulating frequency  $\omega_a$ . In many cases  $\omega_a$  is small, so that  $y \approx 2\Delta\omega\tau$  and the harmonics are proportional to the modulating frequency,  $\omega_a$ . Also, the harmonics are all delayed by  $\tau$  with respect to the recovered signal. Since  $\tau$  is different for different repeater-stations, it follows that there can be no component of distortion adding up in phase from repeater to repeater, and there will be therefore no 'voltage-rise' component of third-harmonic distortion.

These properties of the distortion are different from those which arise when the signal output can be taken as a simple power series expansion of the input. It should not, therefore, be surprising if the absolute value of time delay variation with frequency should turn out not to be a suitable measure of the distortion.

For very short runs,  $y$  is small, and  $J_2(y) \approx y^2/8$ . Hence equation (5) gives, for the second harmonic

$$2r_1 r_2 e^{-2\alpha} \omega_a (\Delta\omega)^2 \tau^2 [\sin(\omega_a \tau) / \omega_a \tau]^2 \sin(2\tau\omega_c - \theta_1 - \theta_2).$$

Apart from the absence of the factor  $[\sin(\omega_a \tau) / \omega_a \tau]^2$  which is usually very close to 1, and the omission of  $\theta_1$  and  $\theta_2$ , this is the same result as can be obtained from the formula for the phase given on p. 62 of Friis's paper (*loc cit.*) by the use of the first few terms of the quasi-stationary-state expansion. But the expression for the variation of time delay with frequency increases proportionally to the length of feeder no matter how long it may be, while  $J_2(y)$  does not rise indefinitely as  $y^2/8$ , but reaches a maximum of about 0.486 at  $y \approx 3$ , whereafter it decreases again and oscillates about zero. For this reason, it is felt that the time-delay variation is not a suitable quantity to use when discussing the distortion arising from feeder mismatches unless the feeder is very short, and conclusions drawn about the unusability of very long feeders may not necessarily be sound.

Unless the feeder length is comparable with the wavelength of the modulating frequency  $\omega_a$ ,  $\omega_a \tau$  will be small, and  $\sin \omega_a \tau / \omega_a \tau$  can be replaced by unity. Hence  $y \approx 2\Delta\omega\tau$ . However, if  $\omega_a \tau = \pi$ ,  $y = 0$  and there is no harmonic distortion whatsoever. This is easily seen to be so from equation (1) since the second term is merely a small multiple of the first, which is accordingly transmitted without phase distortion. This phenomenon will not usually occur for more complex modulating signals, however.

### 5. Example

Consider a wave of r.f. carrier wavelength  $\lambda = 7$  cm, conveyed over a feeder consisting of 50 ft of  $2 \text{ in} \times \frac{3}{8} \text{ in}$  brass waveguide. Let the peak frequency deviation of the modulation be 3 Mc/s, the video band being 800 kc/s wide. It is required to find the distortion at the top of the band. The voltage standing-wave ratios at the ends of the feeder will be taken as 0.95 and 0.65, and the attenuation along the guide as 1 db each way. The group velocity is  $3 \times 10^{10} \cdot \sqrt{1 - \lambda^2/4a^2}$  with  $a = 2$  in.

Hence  $v = 2.1 \times 10^{10}$  cm/sec and  $\tau = 0.71 \times 10^{-7}$  sec.

We use a modulating tone of frequency 0.4 Mc/s in order that its 2nd harmonic may be at the top of the band.

Then  $\omega_a \tau = 2\pi \times 0.4 \times 0.071 = 0.178$  or  $10^\circ$ ,  
 $\sin(\omega_a \tau) / \omega_a \tau = 0.995$

$$y = 2\Delta\omega\tau \cdot \sin(\omega_a \tau) / \omega_a \tau = 2.66 \quad J_2(y) = 0.46$$

$$r_1 r_2 = \frac{1 - 0.95}{1 + 0.95} \cdot \frac{1 - 0.65}{1 + 0.65} = 5.4 \times 10^{-3}$$

$$\therefore \frac{\text{2nd Harmonic}}{\text{Fundamental}} = 5.4 \times 10^{-3} \times (0.8/3) \times 0.45 \times 10^{-0.1} \times \sqrt{2} \equiv 63 \text{ db.}$$

The ratio of third to second harmonic, when each in turn is arranged to occur at the top of the band (by a suitable choice of  $\omega_a$  for each), is  $J_3(2.66)/J_2(2.66) = 0.5$ . The third is thus 6 db down on the second. Since  $J_n(y)$  decreases for  $n$  greater than  $y$ , the higher harmonics rapidly become negligible in this example.

Thus  $J_1(2.66)/J_2(2.66) = 0.17$  which is equivalent to a 15-db margin of fourth to second harmonic.

Equality of third to second would obtain for  $y = 3.75$ ; i.e., for a length of about 70 ft in this example. For greater lengths the second harmonic drops rapidly, becoming zero at 100 ft, the third and subsequently the higher harmonics becoming dominant.

### 6. Connection between Cross-talk and Harmonics

This subject will be dealt with in detail in a forthcoming paper. However, it is obvious from the above example and from Section 4 that the variation of time delay is not a suitable measure of the amount of harmonics produced (except for very small feeder lengths), and it transpires that the harmonic production is equally unsuitable (except in the case of the preponderance of second and third) to describe the cross-talk.

### REFERENCES

- <sup>1</sup> "Micro-wave Repeater Research," by H. T. Friis. *Bell Syst. tech. J.*, April 1948. Vol. 27, pp. 183-246.
- <sup>2</sup> "Variable Frequency Electric Circuit Theory with Application to the Theory of Frequency Modulation," by J. R. Carson and T. C. Fry. *Bell Syst. tech. J.*, October 1937. Vol. 16, pp. 513-540.
- <sup>3</sup> "The Fundamental Principles of Frequency Modulation," by Professor Balhu, van der Pol. *J. Instn. elect. Engrs.*, May 1946. Vol. 93, Part III, pp. 153-158.

# FEEDBACK AMPLIFIERS AND SERVO SYSTEMS

*Their Common Theoretical Basis*

By Edward E. Ward

(The University of Birmingham)

## 1. Introduction

THIS paper, by drawing attention to certain relationships, seeks to show that the distinction between frequency response and transient response which was inevitable in the history of amplifiers and servo systems now threatens to distract attention from facts which are more fundamental—namely, the pattern of poles and zeros of the response function. This pattern might afford a useful basis for classifying and studying these devices since it avoids any cleavage between the frequency function and time function points of view and it appears possible by using the Laplace Transform to sketch out a broader theory which includes them both as special cases. Arguments which hold for feedback amplifiers are in many cases equally true for servo systems since the basic principles of these two devices are alike. The analysis which follows can therefore be applied to both; it will be restricted to linear systems having lumped constants and one closed loop and will be seen to be indebted to the writings of Dr. K. W. Wagner. It is hoped that it will serve as a basis for the extensions and corrections which others will be able to suggest.

## 2. Two Points of View

### 2.1 The Transient Analysis

In negative-feedback amplifiers which meet the conditions stated above, and also similarly in servo systems, having an output voltage  $E_0$  and transmitting an input voltage  $E_i$ , the relations between these quantities may be stated by an equation such as:

$$\begin{aligned} & \left( m_0 + m_1 \frac{d}{dt} + m_2 \frac{d^2}{dt^2} + \dots \right) E_0 \\ & = \left( n_0 + n_1 \frac{d}{dt} + n_2 \frac{d^2}{dt^2} + \dots \right) E_i \end{aligned}$$

This is a linear equation with constant coefficients which may be abbreviated as

$$f_1(D)E_0 = f_2(D)E_i$$

and which may be solved for the transient oscillation by the familiar substitution  $E_0 = Ke^{st}$  in which  $s$  may have to be complex. Putting

$s = u + jv$  the output voltage will be the sum of a number of terms and will have the form

$$E_0 = \Sigma K e^{(u+jv)t}$$

The important point for our present purpose is that this well-known result is similar to the notation whereby an oscillating quantity of angular frequency  $\omega$  is commonly written as the real part of  $Ke^{j\omega t}$  and, in fact, if the coefficients of the equations were such as to represent a system of zero loss and damping, the term  $u$  would vanish in the solution, which would represent a steadily oscillating response of the form  $Ke^{jvt}$ .

### 2.2 The Frequency Analysis.

This treatment, unlike that given above, concentrates on the performance of the system under sinusoidal signals. For an input oscillation  $E_i$  having an angular frequency  $\omega$  at which the forward and feedback chains have amplifications  $\mu$  and  $\beta$  respectively, the output oscillation

$$\text{will be: } E_0 = \left( \frac{\mu}{1 + \mu\beta} \right) E_i$$

In this equation all the terms may be complex: the response of the system, defined as the Transfer Function  $Y$ , or the complex quotient  $E_0/E_i$ , is found by working out the modulus and argument of the expression in brackets; the design methods based on the Nyquist diagram demand not only a knowledge of the values of the complex quantity  $\mu\beta$  but an ability to control its variation as a function of  $\omega$  in the manner required.

Here is the crux of the matter for the designer. His task is to obtain effective design control over the modulus and argument of the product  $\mu\beta$ . If we take  $G_1$  to be the loop gain in nepers and  $\phi_1$  the loop phase shift in radians then

$$\log(\mu\beta) = \log|\mu\beta| + j \text{Arg}(\mu\beta) = G_1 + j\phi_1$$

The practical difficulty is that  $G_1$  and  $\phi_1$  are not independent; with a few exceptions, a change in one must affect the other; their inter-dependence is, in most practical systems, of a complicated and elusive kind.

The principle which governs this inter-dependence is, however, not a complicated one and is best understood by starting with a simple case such as the circuit shown in Fig. 1. If an input

voltage  $E_i\sqrt{2} \sin \omega t$  be applied to this circuit in which the inductance is  $L$  and the resistance  $R$  then the open-circuit voltage  $E_0$  at the output terminals is given by

$$E_0 = \left( \frac{R}{R + j\omega L} \right) E_i \dots \dots \dots (1)$$

and if the response be written as

$$\frac{E_0}{E_i} = |Y|e^{j\phi} \text{ with } \frac{R}{L} = \omega_0 \text{ then}$$

$$|Y| = \frac{\omega_0}{\sqrt{\omega_0^2 + \omega^2}}; \phi = -\tan^{-1}\left(\frac{\omega}{\omega_0}\right)$$

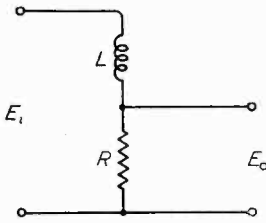
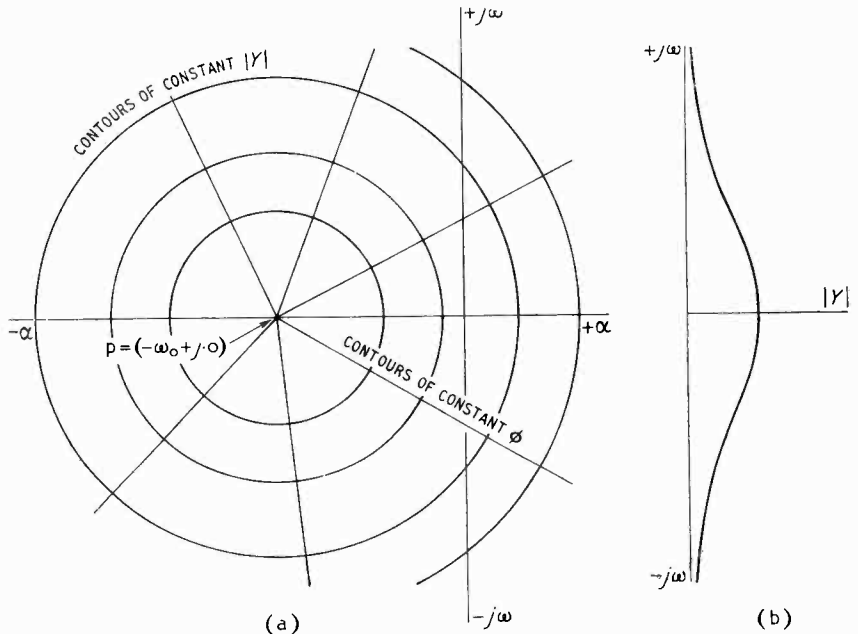


Fig. 1 (above). Circuit represented by Equ. (1).

Fig. 2 (right). Pole of a response function (a), and the variation of  $|Y|$  along the  $j\omega$  axis (b).



In this form as functions of  $\omega$  the above expressions for  $|Y|$  and  $\phi$  do not suggest that they are related in any simple way. However, if we write  $E_i\sqrt{2} \sin \omega t$  as the real part of  $E_i\sqrt{2}e^{j\omega t}$  and regard  $j\omega$  as the imaginary term of a complex variable  $(\alpha + j\omega)$  then we have

$$|Y| = \frac{\omega_0}{\sqrt{(\omega_0 + \alpha)^2 + \omega^2}}$$

$$\phi = -\tan^{-1}\left(\frac{\omega}{\omega_0 + \alpha}\right)$$

If contours of constant  $|Y|$  and  $\phi$  be plotted in the plane of  $(\alpha + j\omega)$  they appear as concentric circles and as radii respectively, disposed as in Fig. 2(a) about a centre at  $(\alpha = -\omega_0, j\omega = 0)$ . Equation (1) which, in this complex plane, has a meaning only on the  $j\omega$  axis, may be rewritten as

$$E_0 = \left[ \frac{R}{R + (\alpha + j\omega)L} \right] E_i$$

$$\text{or } E_0 = \left[ \frac{\omega_0}{\omega_0 + p} \right] E_i \dots (2)$$

where  $p$  is the complex quantity  $p = \alpha + j\omega$ .

Equation (2) shows that the quotient  $\left(\frac{E_0}{E_i}\right)$  has a

pole (i.e., it tends to infinity) at  $p = (-\omega_0 + j.0)$  and this simple example shows that the obscure connection between  $|Y|$  and  $\phi$  as found by sine-wave measurements (that is, on the  $j\omega$  axis where  $\alpha = 0$ ) is that they are both obliged to vary in the manner determined by the pole of the response function. This pole is not to be found on the  $j\omega$  axis but is at the point  $p = (-\omega_0 + j.0)$  in the complex plane. This is shown in Fig. 3 where the height of the solid figures represents  $|Y|$ . The value of  $|Y|$  for sine waves, for which  $\alpha = 0$ , is represented by the section cut in the solid

figure by the plane containing the  $j\omega$  axis and this section is shown in Fig. 2(b).

Finally, by taking logarithms, we have

$$N = G + j\phi = \log\{|Y|e^{j\phi}\} = \log\{f(\alpha + j\omega)\}$$

which is the fundamental relation between gain and phase, showing them to be conjugate functions of the complex variable  $(\alpha + j\omega)$ . This means that  $G$ , the gain in nepers, and  $\phi$ , the phase rotation in radians, are real quantities which are free to vary only in certain inter-dependent ways; their mutual relation must be such that the complex variable  $N = (G + j\phi)$  will always have a finite differential coefficient with respect to the complex variable  $p = (\alpha + j\omega)$  of which it will be an analytic function. Contours of constant  $G$  and of constant  $\phi$  will then intersect orthogonally when mapped in the plane of  $(\alpha + j\omega)$ . Although the above example is a simple one it will appear later that the gain and phase of more complicated structures having several poles and zeros are, with certain exceptions, related in a closely

similar manner when regarded as functions of  $(\alpha + j\omega)$ .

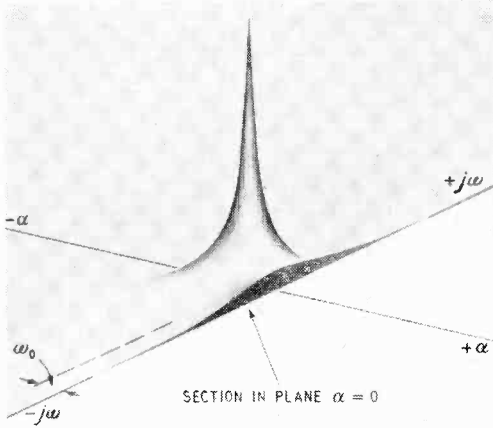


Fig. 3. This solid figure represents the contours of Fig. 2(a).

### 3. Pattern of Poles and Zeros §

We can therefore see that the exponential way of representing an oscillation as  $Ae^{j\omega t}$  may usefully be extended as  $Ae^{(\alpha+j\omega)t}$  and that this latter form not only represents the possible responses to a transient but also brings to light the underlying reasons for behaviour which is observed under sinusoidal signals and represented along the  $j\omega$  axis. The handy name Complex Frequency has quite wrongly crept into use for the variable  $p = (\alpha + j\omega)$  and needs attention from those who watch over our nomenclature. The idea itself, however, is clearly important and we must now show how it can be used.

The instance taken above shows how the response  $\left(\frac{\omega_0}{\omega_0 + j\omega}\right)$  to an oscillation  $Ae^{j\omega t}$  becomes  $\left(\frac{\omega_0}{\omega_0 + [\alpha + j\omega]}\right)$  to an oscillation  $Ae^{(\alpha+j\omega)t}$  and in general the transfer function of a complicated system may be written as

$$|Y|e^{j\phi} = \left(\frac{E_0}{E_i}\right) = \left[\frac{(p+a_1)(p+a_2)(\dots)}{(p+b_1)(p+b_2)(\dots)}\right] \quad (3)$$

a quotient which has poles at  $-b_1, -b_2$  etc., and zeros at  $-a_1, -a_2$ , etc., where some of the  $a$  and  $b$  terms may be real and some complex; since the coefficients are real, complex roots will appear only in conjugate pairs. The modulus and argument of  $|Y|e^{j\phi}$  vary from point to point in the plane of  $p = \alpha + j\omega$  and depend only on the positions of the poles and zeros of the function. When the transfer function is extended in this

§ See, for example: E. G. Phillips: "Functions of a Complex Variable"; Oliver & Boyd, 1947.

way to have a meaning for signals of the form  $Ae^{(\alpha+j\omega)t}$  it is called a Laplace Transform.

An impedance or admittance which is a function of the variable  $j\omega$  may similarly be extended as a function of  $(\alpha + j\omega)$ . For example, if the current in an inductance be  $Ie^{j\omega t}$  then the product  $Ldi/dt$  will have the value  $LIj\omega e^{j\omega t}$  giving an impedance  $j\omega L$ ; whereas if the current be  $Ie^{(\alpha+j\omega)t}$  then  $Ldi/dt$  will become  $LI(\alpha + j\omega)e^{(\alpha+j\omega)t}$  giving an impedance  $(\alpha + j\omega)L$  which is again a Laplace Transform.

From this point we can see how the frequency performance and the transient performance of a feedback amplifier or a servo-system can be built up from the pattern of poles and zeros of the response function.

#### 3.1 Performance as a Frequency Function :

For simplicity we may allow ourselves to speak of the poles and zeros of a system when strictly we mean that they belong to an equation. Thus we say that a system having a single pole at  $\alpha = -\omega_0$  will have a transfer function

$$Y_{(p)} = \left(\frac{\omega_0}{p + \omega_0}\right)$$

and for sinusoidal oscillations

$$Y_{(j\omega)} = \left(\frac{\omega_0}{j\omega + \omega_0}\right)$$

of which we have already found the modulus and argument. Likewise, for a system of two poles :

$$Y_{(j\omega)} = \frac{a_1}{(j\omega + b_1)(j\omega + b_2)}$$

In the general case, the modulus and argument of the response are the values given by the Laplace Transform when  $p$  is purely imaginary; from Equ. (3) these are :

$$|Y|_{(j\omega)} = \left|\frac{E_0}{E_i}\right| = \left\{ \frac{|j\omega + a_1| \times |j\omega + a_2| \times \dots}{|j\omega + b_1| \times |j\omega + b_2| \times \dots} \right\}$$

$$\phi_{(j\omega)} = \text{Arg} E_0 - \text{Arg} E_i = \Sigma \text{Arg}(j\omega + a_n) - \Sigma \text{Arg}(j\omega + b_n)$$

and the gain of the system may be found by adding algebraically the components due to each pole and zero :

$$G = \log |Y| = \Sigma \log |j\omega + a_n| - \Sigma \log |j\omega + b_n|$$

The poles of the transfer function of equation (3) are the zeros of the function  $(1 + \mu\beta)$  and a convenient practical technique at present in use consists in applying the above analysis to the product  $\mu\beta$  which is similarly a rational function of  $p$  and of which  $G_1$  and  $\phi_1$  may be displayed in a Nyquist diagram as functions of  $j\omega$ .

#### 3.2 Response to a Transient

The importance of the complex variable  $p = (\alpha + j\omega)$  in predicting the response to a

transient is a result of the difficulty of representing a transient in mathematical terms. Repeating oscillations of complicated shapes may be represented by Fourier series, consisting of terms of the form  $Ae^{j\omega t}$ , but however small the angular frequency  $\omega$  may be, the oscillations go on indefinitely whereas a transient happens only once. This is not surprising since the Fourier series contain no mechanism to provide for the dying away of the components which form the sum. Of the several possible devices, that used in the Laplace Transform consists in assembling the transient from the 'terms' of a Fourier integral—that is, a Fourier series having its terms infinitely close together in frequency—of which the 'terms' are multiplied by a decay factor  $e^{-\alpha t}$ . The transient is therefore assembled from oscillations of the form  $Ae^{(\alpha+j\omega)t}$ .

The magnitude of any chosen component  $Ae^{j\omega t}$  of a Fourier series is found by integrating over one cycle the product of the time function  $f(t)$  and a multiplier  $e^{-j\omega t}$  which holds the required term constant while the other terms perform complete cycles of which the integrals vanish. Similarly the magnitude (more precisely, the complex amplitude function) of any chosen component  $A \cdot d\phi \cdot e^{(\alpha+j\omega)t}$  of the Laplace Transform is found by integrating over one cycle (there is only one; i.e., from  $t=0$  to  $t=+\infty$ ) the product  $f(t) \times e^{-(\alpha+j\omega)t} = f(t) e^{-pt}$ . If the transform exists, the real part of  $p$  must not fall below a certain value, known as the Abscissa of Convergence, in order to make the integral convergent.

As in a Fourier series, the integral  $\int_0^{\infty} f(t) \cdot e^{-pt} \cdot dt$  answers the question, "How strong is the component oscillation of the form  $e^{pt} d\phi$ ?" and the answer it gives depends, of course, on the value of  $p$  in the question. This means that for a given transient input signal  $E_i$  the Laplace Transform is a function which shows the strength in that particular transient of the component oscillations of form  $e^{pt} d\phi$  and the manner in which it depends on  $p$  and  $K$ . W. Wagner has clinched the matter by calling it the Frequency Spectrum of the transient.†

We are now within sight of our goal. For we have already seen that an impedance function or a response function of an electrical system—and, equally, of a mechanical system—to oscillations of precisely this form is a function of its poles and zeros in the plane of  $p$  and is also known as a Laplace Transform. The output signal of the system will, therefore, consist of a spectrum of incremental oscillations, each of the form  $A \cdot d\phi \cdot e^{(\alpha+j\omega)t}$ , where for every value of  $p$  the coefficient  $A$  will be the product

of the strength of that oscillation in the original signal (i.e.,  $\mathcal{L}E_i$ ) and the amplification or attenuation and phase-shift applied to it by the system (i.e.,  $Y_{(p)}$ ). In order to find the output we have to add these oscillations.

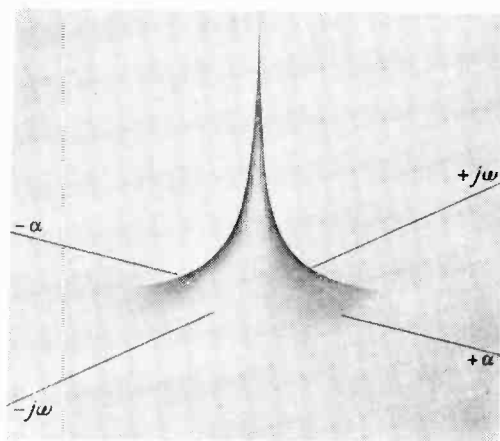


Fig. 4. Laplace transform of a step function; the amplitude of any given component is represented by the height of the solid figure.

A concrete example will help here and we may attempt the response of an elementary amplifier or servo system having a second-order equation and subject to a step-function. Using the symbols  $\mathcal{L}E_i$  to represent the step-function we know that its 'frequency spectrum' or Laplace Transform is  $\mathcal{L}\mathcal{L}E_i = E_i/p$  meaning that the incremental oscillations lying between  $e^{pt}$  and  $e^{(p+d\omega)t}$  have a complex amplitude  $(E_i \cdot d\phi)/p$ . This function has a simple pole at the origin and is otherwise analytic. It is shown graphically in Fig. 4. The transfer function of the system for oscillations  $Ae^{pt}$  will be

$$Y_{(p)} = \left( \frac{E_0}{E_1} \right)_{(p)} = \frac{F^2}{p^2 + 2Kp + F^2}$$

and the 'frequency spectrum' of the output oscillations will therefore be

$$\mathcal{L}E_0 = \left( \frac{F^2}{p^2 + 2Kp + F^2} \right) \cdot \frac{E_i}{p}$$

which may be factorised as

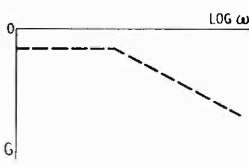
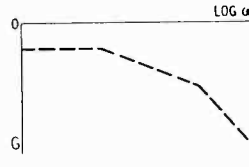
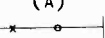
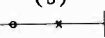
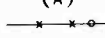
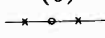
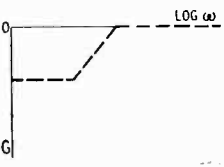
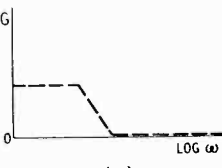
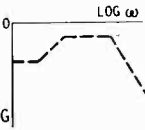
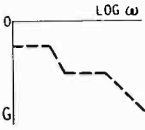
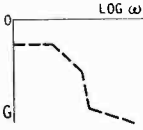
$$\mathcal{L}E_0 = \left( \frac{F^2}{p(p+b_1)(p+b_2)} \right) E_i \quad \dots \quad (4)$$

One of the possible dispositions of this output transform is shown graphically in Fig. 5. The output is given by adding all the oscillations whose amplitudes are shown in Fig. 5, along the line from  $c - j\infty$  to  $c + j\infty$ , the real part  $\alpha$  being held to a certain minimum value  $c$  as will appear later.

The process of adding these oscillations, that is, of integrating a function of a complex variable,

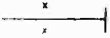
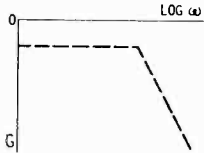
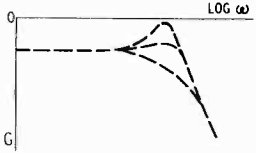
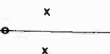
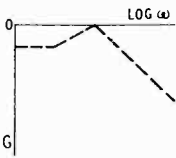
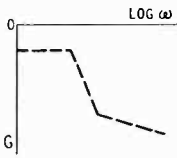
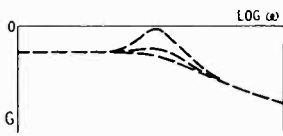
† "Operatorenrechnung": p. 28; Leipzig, 1940.

# TENTATIVE CLASSIFICATION

	ONE REAL POLE	TWO REAL POLES
(a)		
	$Y = \frac{1}{(p + b_1)}$	$Y = \frac{1}{(p + b_1)(p + b_2)}$
(c)	$Y = \frac{1}{(j\omega + b_1)}$	$Y = \frac{1}{(j\omega + b_1)(j\omega + b_2)}$
(d)	$\log  Y  = - \left\{ \log b_1 + \log \left  1 + \frac{j\omega}{b_1} \right  \right\}$	$\log  Y  = - \left\{ \log b_1 b_2 + \log \left  1 + \frac{j\omega}{b_1} \right  + \log \left  1 + \frac{j\omega}{b_2} \right  \right\}$
(e)	$\text{Arg } Y = - \tan^{-1} \left( \frac{\omega}{b_1} \right)$	$\text{Arg } Y = - \left\{ \tan^{-1} \left( \frac{\omega}{b_1} \right) + \tan^{-1} \left( \frac{\omega}{b_2} \right) \right\}$
(f)	$f(t) = A_1 (1 - e^{-b_1 t})$	$f(t) = A_1 + A_2 e^{-b_1 t} + A_3 e^{-b_2 t}$
(g)		
(a)	<div style="display: flex; justify-content: space-around;"> <div style="text-align: center;">(A) </div> <div style="text-align: center;">(B) </div> </div>	<div style="display: flex; justify-content: space-around;"> <div style="text-align: center;">(A) </div> <div style="text-align: center;">(B) </div> <div style="text-align: center;">(C) </div> </div>
(b)	$Y = \frac{(p + a_1)}{(p + b_1)}$	$Y = \frac{(p + a_1)}{(p + b_1)(p + b_2)}$
(c)	$Y = \frac{(j\omega + a_1)}{(j\omega + b_1)}$	$Y = \frac{(j\omega + a_1)}{(j\omega + b_1)(j\omega + b_2)}$
(d)	$\log  Y  = \left[ \log a_1 + \log \left  1 + \frac{j\omega}{a_1} \right  \right] - \left[ \log b_1 + \log \left  1 + \frac{j\omega}{b_1} \right  \right]$	$\log  Y  = \left\{ \log a_1 + \log \left  1 + \frac{j\omega}{a_1} \right  \right\} - \left\{ \log b_1 b_2 + \log \left  1 + \frac{j\omega}{b_1} \right  + \log \left  1 + \frac{j\omega}{b_2} \right  \right\}$
(e)	$\text{Arg } Y = \tan^{-1} \left( \frac{\omega}{a_1} \right) - \tan^{-1} \left( \frac{\omega}{b_1} \right)$	$\text{Arg } Y = \tan^{-1} \left( \frac{\omega}{a_1} \right) - \tan^{-1} \left( \frac{\omega}{b_1} \right) - \tan^{-1} \left( \frac{\omega}{b_2} \right)$
(f)	$f(t) = A_1 - A_2 e^{-b_1 t}$	$f(t) = A_1 + A_2 e^{-b_1 t} + A_3 e^{-b_2 t}$
(g)	<div style="display: flex; justify-content: space-around;"> <div style="text-align: center;">(A) </div> <div style="text-align: center;">(B) </div> </div>	<div style="display: flex; justify-content: space-around;"> <div style="text-align: center;">(A) </div> <div style="text-align: center;">(B) </div> <div style="text-align: center;">(C) </div> </div>

(a) Pattern of  $p$ -plane      (b) Laplacian form of response      (c) Sinusoidal form of response

# OF RESPONSE FUNCTIONS

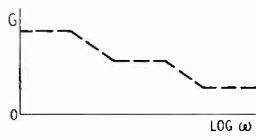
TWO COINCIDENT POLES	TWO COMPLEX POLES	
		(a)
$Y = \frac{I}{(p + b_1)^2}$	$Y = \frac{I}{[p + (\alpha_0 + j\omega_0)][p + (\alpha_0 - j\omega_0)]}$	(b)
$Y = \frac{I}{(j\omega + b_1)^2}$	$Y = \frac{I}{[-\omega^2 + 2j\omega\alpha_0 + (\alpha_0^2 + \omega_0^2)]}$	(c)
$\log  Y  = -2 \left\{ \log b_1 + \log \left  1 + \frac{j\omega}{b_1} \right  \right\}$	$\log  Y  = -\log  (\omega_0^2 + \alpha_0^2 - \omega^2) + 2j\omega\alpha_0 $	(d)
$\text{Arg } Y = -2 \tan^{-1} \left( \frac{\omega}{b_1} \right)$	$\text{Arg } Y = -\tan^{-1} \left( \frac{2\omega\alpha_0}{\alpha_0^2 + \omega_0^2 - \omega^2} \right)$	(e)
$f(t) = A_1 \{ 1 - (1 + b_1 t) e^{-b_1 t} \}$	$f(t) = A_1 + A_2 e^{-\alpha_0 t} \sin(\omega_0 t + A_3)$	(f)
		(g)
<div style="display: flex; justify-content: space-around;"> <div data-bbox="202 1009 313 1062">(A) </div> <div data-bbox="431 1009 542 1062">(B) </div> </div>		(a)
$Y = \frac{(p + a_1)}{(p + b_1)^2}$	$Y = \frac{(p + a_1)}{[p + (\alpha_0 + j\omega_0)][p + (\alpha_0 - j\omega_0)]}$	(b)
$Y = \frac{(j\omega + a_1)}{(j\omega + b_1)^2}$	$Y = \frac{(j\omega + a_1)}{[-\omega^2 + 2j\omega\alpha_0 + (\alpha_0^2 + \omega_0^2)]}$	(c)
$\log  Y  = \left\{ \log a_1 + \log \left  1 + \frac{j\omega}{a_1} \right  \right\} - 2 \left\{ \log b_1 + \log \left  1 + \frac{j\omega}{b_1} \right  \right\}$	$\log  Y  = \log a_1 + \log \left  1 + \frac{j\omega}{a_1} \right  - \log  (\omega_0^2 + \alpha_0^2 - \omega^2) + 2j\omega\alpha_0 $	(d)
$\text{Arg } Y = \tan^{-1} \left( \frac{\omega}{a_1} \right) - 2 \tan^{-1} \left( \frac{\omega}{b_1} \right)$	$\text{Arg } Y = \tan^{-1} \left( \frac{\omega}{a_1} \right) - \tan^{-1} \left( \frac{2\omega\alpha_0}{\alpha_0^2 + \omega_0^2 - \omega^2} \right)$	(e)
$f(t) = A_1 + (A_2 t - A_1) e^{-b_1 t}$	$f(t) = A_1 + A_2 e^{-\alpha_0 t} \sin(\omega_0 t + A_3)$	(f)
<div style="display: flex; justify-content: space-around;"> <div data-bbox="168 1434 343 1591">  <p>(A)</p> </div> <div data-bbox="405 1434 580 1591">  <p>(B)</p> </div> </div>		(g)

(d) Gain

(e) Phase

(f) Step-function response

(g) Gain profiles

	ONE REAL POLE	TWO REAL POLES
(a)		 and other patterns
(b)	$Y = \frac{(p + a_1)(p + a_2)}{(p + b_1)}$	$Y = \frac{(p + a_1)(p + a_2)}{(p + b_1)(p + b_2)}$
(c)		$Y = \frac{(j\omega + a_1)(j\omega + a_2)}{(j\omega + b_1)(j\omega + b_2)}$
(d)	NOT FOUND	$\log  Y  = \left\{ \log  a_1 a_2  + \log \left  1 + \frac{j\omega}{a_1} \right  + \log \left  1 + \frac{j\omega}{a_2} \right  \right\} - \left\{ \log  b_1 b_2  + \log \left  1 + \frac{j\omega}{b_1} \right  + \log \left  1 + \frac{j\omega}{b_2} \right  \right\}$
(e)		$\text{Arg } Y = \left\{ + \tan^{-1} \left( \frac{\omega}{a_1} \right) + \tan^{-1} \left( \frac{\omega}{a_2} \right) \right\} - \left\{ \tan^{-1} \left( \frac{\omega}{b_1} \right) + \tan^{-1} \left( \frac{\omega}{b_2} \right) \right\}$
(f)		$f(t) = A_1 + A_2 e^{-b_1 t} + A_3 e^{-b_2 t}$
(g)		 and other profiles

(a) Pattern of  $p$ -plane

(b) Laplacian form of response

(c) Sinusoidal form of response

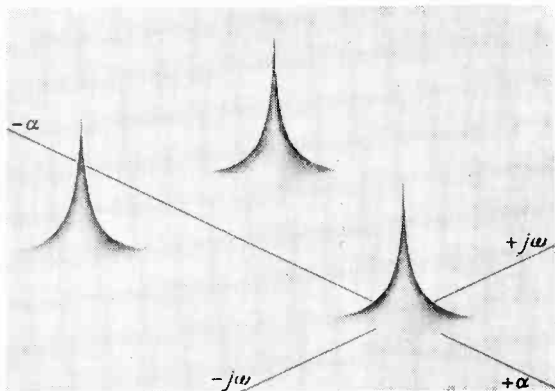


Fig. 5. Laplace transform of output.

is almost impossible to grasp without some kind of physical analogue; perhaps the most graphic of these is a large shallow sink provided with a plug-hole at each zero of the plane and a running tap at each pole. The function of equation (4) has one pole at the origin and two other poles which may be disposed in certain ways in the negative half plane. The integral for  $t < 0$  is taken over the positive half plane; the hydraulic analogy is in agreement in that the

total flow over a closed contour which does not enclose either sources or sinks is zero. The integral for  $t > 0$  is taken over the negative half plane in the manner shown in Fig. 6 and the constant value of  $\alpha = c$  is taken to ensure that all the poles and zeros—corresponding to sources and sinks—are enclosed. Analytically, the integral is written

$$E_0 = \frac{1}{2\pi j} \int_{c-j\infty}^{c+j\infty} \frac{E_i \cdot F_2 e^{pt}}{p(p+b_1)(p+b_2)} \cdot dp$$

$$= \frac{E_i}{2\pi j} \int_{c-j\infty}^{c+j\infty} e^{pt} \left[ \frac{F_1}{p} + \frac{F_2}{(p+b_1)} + \frac{F_3}{(p+b_2)} \right] \cdot dp$$

and the familiar result is seen to contain a characteristic contribution from each pole or pair of conjugate poles of the response function. The final form of the output is governed by the values of  $b_1$  and  $b_2$  but one possible response is given by

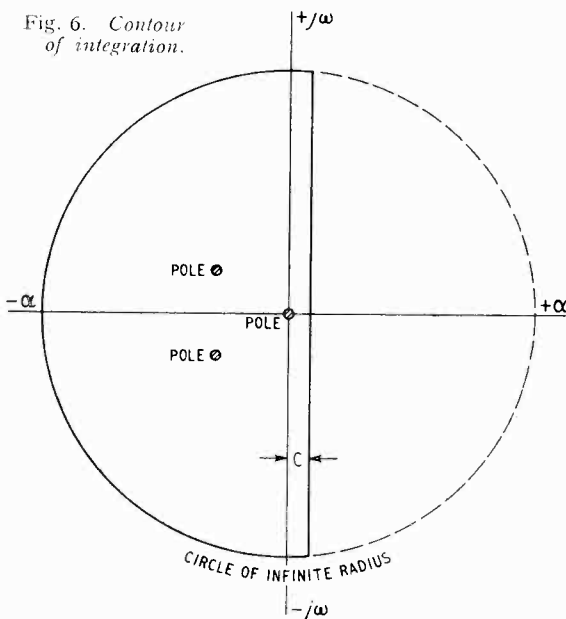
$$E_0 = E_i \left\{ 1 - K_1 e^{b_1 t} + K_2 e^{b_2 t} \right\}$$

#### 4. Tentative Classification

Without attempting a rigorous mathematical proof, we have shown that poles and zeros of a rational function are the only elements available for building the response functions of such systems as we are examining. It is therefore

TWO COINCIDENT POLES	TWO COMPLEX POLES
$Y = \frac{(p + a_1)(p + a_2)}{(p + b_1)^2}$ $Y = \frac{(j\omega + a_1)(j\omega + a_2)}{(j\omega + b_1)^2}$	$Y = \frac{(p + a_1)(p - a_2)}{[p + (\alpha_0 + j\omega_0)][p + (\alpha_0 - j\omega_0)]}$ $Y = \frac{(j\omega + a_1)(j\omega + a_2)}{[(-\omega^2 + 2j\omega\alpha_0 + (\alpha_0^2 + \omega_0^2))]}$
$\log  Y  = \left\{ \log  a_1 a_2  + \log \left  1 + \frac{j\omega}{a_1} \right  + \log \left  1 + \frac{j\omega}{a_2} \right  - 2 \left\{ \log b_1 + \log \left  1 + \frac{j\omega}{b_1} \right  \right\} \right.$	$\log  Y  = \left\{ \log a_1 a_2 + \log \left  1 + \frac{j\omega}{a_1} \right  + \log \left  1 + \frac{j\omega}{a_2} \right  - \log  (\omega_0^2 + \alpha_0^2 - \omega^2) + 2j\omega\alpha_0  \right\}$
$\text{Arg } Y = \left\{ + \tan^{-1} \left( \frac{\omega}{a_1} \right) + \tan^{-1} \left( \frac{\omega}{a_2} \right) - 2 \tan^{-1} \left( \frac{\omega}{b_1} \right) \right\}$	$\text{Arg } Y = \left\{ \tan^{-1} \left( \frac{\omega}{a_1} \right) + \tan^{-1} \left( \frac{\omega}{a_2} \right) - \tan^{-1} \left( \frac{2\omega\alpha_0}{\alpha_0^2 + \omega_0^2 - \omega^2} \right) \right\}$
$f(t) = A_1 + (A_2 t + A_3) e^{-b_1 t}$	$f(t) = A_1 + A_2 e^{-\alpha_0 t} \sin(\omega_0 t + A_3)$
(d) Gain	(e) Phase
(f) Step-function response	(g) Gain profiles

Fig. 6. Contour of integration.



clear that—with certain exceptions—a given triad of gain, phase and transient functions, generated by a given pattern of poles and zeros,

can only make a joint appearance and will not be found in other arrangements. Thus the pattern of the singularities in the  $p$ -plane is a logical basis for classifying these systems and the summary of known results which appears in the accompanying Table should make it possible to estimate the uses and limitations of the scheme and to extend it. The response functions met in real amplifiers and servo systems are usually more complicated than any shown in the Table but their gain, phase and transient responses may all be assembled from those elements which are shown.

The next task in integrating the theory of linear closed-loop systems is to show how to provide a computing device whereby the gain, phase and transient functions may be given immediately in terms of the singularities in the complex plane. Work is now under way on such a device, following the lines sketched above.

## 5. Acknowledgment

The author wishes to acknowledge his debt to the interest and encouragement of Prof. A. Tustin and of his other colleagues in the Electrical Engineering Department of the University of Birmingham.

# IMPEDANCE MEASUREMENT

*Comparison Method with C. R. Indicator*

By H. J. Round

A SIMPLE method of determining impedance and admittance values over ranges of frequency from 1,000 c/s to 150,000 c/s and impedance values from two or three ohms up to two or three hundred ohms is described. It was used at certain Naval Establishments during the war because beat-frequency oscillators (b.f.o.) and normal cathode-ray oscilloscopes (c.r.o.) with attached amplifiers were available. Being earthy instruments they did not lend themselves easily to bridge schemes without the introduction of carefully arranged transformers. It was consequently decided to try out a comparison method.

## General Principle

The general principle employed is to establish a constant-current condition from the b.f.o. and for small currents this is done by using a swamping resistance, of about 100 times the value of the unknown impedance in series with it. The c.r.o. is then used as a voltage indicator to compare and equalize the voltages across the impedance and an adjustable resistance when these are placed in turn in series with the swamping resistance. The balancing resistance used is obtained from an ordinary non-inductive re-

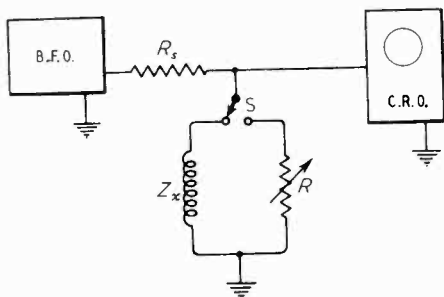


Fig. 1. General arrangement of comparison method:  $R_s$  is the swamping resistance to give constant current,  $Z_x$  the unknown impedance and  $R$  a resistance box.

sistance box and Fig. 1 shows the simple arrangement in which the double-throw switch  $S$  enables one to set the resistance value in the box to give the same deflection on the c.r.o. as the unknown impedance. A big deflection on the c.r.o. is obviously a requirement for accuracy and the c.r.o. amplifier can be adjusted at will to keep deflection

large. Voltage supply from the b.f.o. can also be varied according to requirements.

It will be seen that one has now obtained a resistance value  $R$  equal to the scalar value of the impedance and that the vector angle is still unknown. If now a known impedance, say either a resistance  $R''$  or a reactance, is connected with the unknown, either in series or in parallel, and a new balancing value of resistance  $R'$  determined sufficient data is obtained to evaluate the vector angle graphically or by calculation. Fig. 2 shows the addition of a known resistance  $R''$  in series with the unknown impedance.

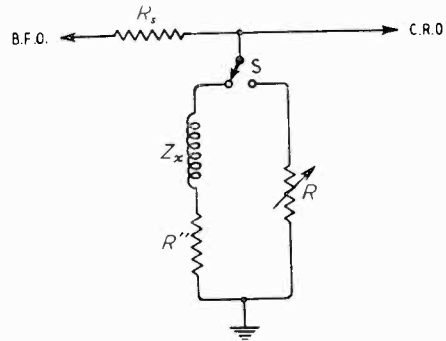


Fig. 2. A second measurement with the addition of  $R''$  enables the phase angle of  $Z_x$  to be determined.

## Details of Method

Consider the measurement of an inductive reactance such as a coil wrapped round a ferromagnetic core.

Suppose  $Z_x$  in Fig. 1 represents such a coil; the first measurement gives the scalar value  $R$  of the impedance of  $Z_x$  and all that can be stated is that the vector end lies somewhere on the circle  $A$  of radius equal to the impedance  $Z_x$ ; that is, of radius equal to the balancing resistance  $R$  as in Fig. 3(a).  $OX$  and  $OY$  represent the resistive and reactive axes respectively.

The resistance  $R''$  of about equal value to the impedance  $Z_x$  is now connected in series with the unknown and a new balancing-resistance value  $R'$  obtained. This enables us to draw a second circle  $A'$  of radius  $R'$  Fig. 3(b).

To see clearly what is happening let us suppose  $OV$  represents the actual vector of  $Z_x$ . To this we have added resistance  $R''$  and in Fig. 3(b) this resistance is shown as  $VV'$ . The combined vector is now shown as  $OV'$ . If we draw a line

$VO'$  parallel to  $V'O$  then  $OO'$  will also represent the added resistance  $R''$  and  $O'V$  will also equal the combined vector.

It is easy now to see the construction to use Fig. 3(c). The first circle is struck with radius  $R$ , then  $OO'$  is set out on the X axis negatively from  $O$  and equal to  $R''$ , and finally a new circle is struck with centre  $O'$  with radius  $R'$  cutting the first circle at  $V$  and  $V_1$ .

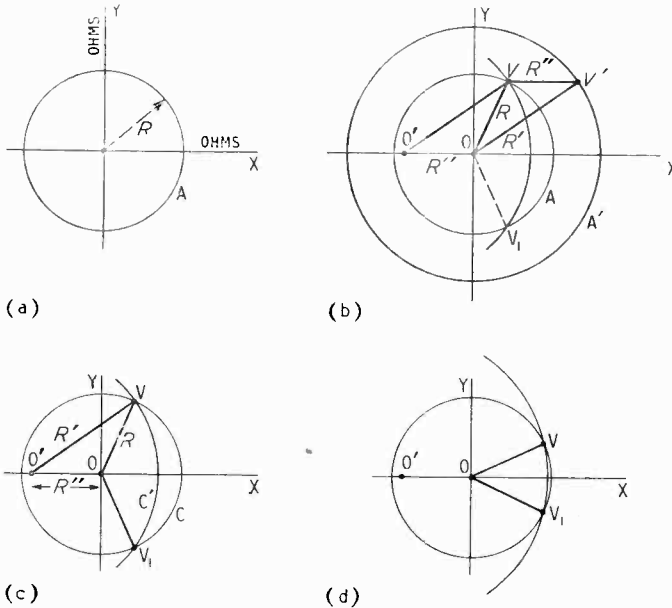


Fig. 3. A single measurement, giving the magnitude of  $Z_x$  as  $R$ , enables only the circle  $A$  to be drawn as in (a). A second measurement with  $R''$  added provides a second circle  $A'$  as in (b), and then the vector  $OV$  can be determined. The construction to find the vector is shown in (c) while the difficulty which occurs when  $Z_x$  has a large resistive component is illustrated in (d).

Quite definitely we can now say that the unknown is either  $OV$  or  $OV_1$ , usually other knowledge of the unknown will enable one to pick the right one of these two solutions. It will be noted that no calculations are necessary, a pair of compasses and some graph paper being the only requirements.

### Improved Method

Experience with this method very soon showed up serious faults.

If  $R''$  is chosen as a rather small value the cutting angle of the two circles is very acute and point  $V$  is not very well defined. If  $R''$  is chosen as a large value it will be easily seen that there is a possible greater error in the reading of  $O'V$ —again making  $V$  difficult to determine accurately.

Reactances with large resistive values give very indeterminate readings owing to the narrow cutting angles of the two circles, a case of this is illustrated in Fig. 3(d). The method was then revised and instead of inserting a known resistance  $R''$  a known high-quality mica capacitor  $C$ , of impedance value approximately the same as the unknown, was inserted as shown in Fig. 4.

The construction of the diagram Fig. 5 is very similar but now the point  $O'$  is marked off on the vertical axis, with  $OO'$  equal to the added capacitive reactance. It will be seen in Fig. 5 that the cutting angle of the two circles  $A$  and  $A'$  is a very good one for defining point  $V$ , right up to the point where  $V$  may be on the X axis.

The assumption is made of course that the mica capacitor is practically lossless.

An examination of Fig. 5 shows that for determining vectors which are capacitive, an added inductance of low loss is advisable to maintain a good cutting angle but the use of an added inductance was not developed very far as most of the measurements required were obtainable with added capacitors.

The two arcs  $A''$  and  $A'''$  show how the circle cutting angle decreases as the vector  $O'V$  increases until in the case of  $A'''$  considerable error could be introduced. Here obviously if the point  $O''$  were chosen as the centre of the second circle the cutting angle would

be good.  $OO''$  represents the addition of an inductance.

### Apparatus

#### Switching

A switching system was evolved which is shown basically in Fig. 6 with the switches marked  $S_1$  to  $S_4$ .

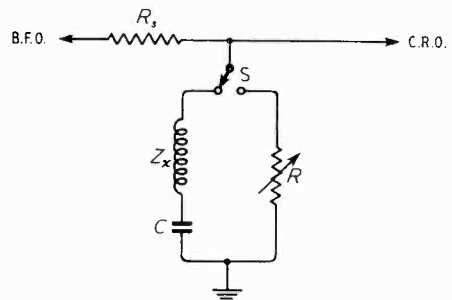


Fig. 4. Here the second measurement is taken with a capacitance  $C$  inserted in series with  $Z_x$ .

$S_1$  = double-pole double-throw switch for comparison purposes.

$S_2$  = double-pole single-throw switch to put the unknown in position for measuring.

$S_3$  = double-pole single-throw switch to insert the capacitor for setting and measurement.

$S_4$  = double-pole single-throw switch for inserting the capacitor in series with the unknown for the second vector measurement.

### Operation

Using  $S_1$  for comparison.

With  $S_2$  thrown, the scalar value  $R$  is determined.

With  $S_3$  thrown a capacitor is chosen with a scalar value  $R''$  about equal to  $R$  or  $Z_x$ .

With  $S_4$  thrown the combined scalar value  $R'$  is obtained.

On the graph sheet the position of the vector can then be at once marked.

It will be noted that the exact value of the capacitor need not be known as its reactance is determined in the operation with  $S_3$ .

It is nearly always most convenient to make the reactance of  $C$  equal to the unknown impedance; i.e., to  $R$ . This in general gives the best cutting angle and also speeds up the measurement.

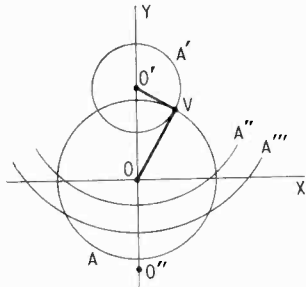


Fig. 5. The construction to determine the vector when capacitance is added is shown.

### Notes on Measurements

If the impedance being measured is not very resistive the second circle is small in diameter and the c.r.o. deflection will on the same scale be small and difficult to read accurately. This can be countered in the measurement by either increasing the b.f.o. voltage or increasing the c.r.o. amplification. In fact, the tendency is always to work to a large fixed deflection marked on the c.r.o. tube. Incidentally waveform can be watched during the operations, and if this gets seriously away from a sine wave, filters can be inserted, unless, of course, the non-linearity is caused by the unknown.

Actually a simple capacitor to earth, connected part of the way along the swamping resistance from the b.f.o., can be made to provide sufficient filtering of harmonics.

A little later on the question of admittance measurement is discussed, and it is sometimes a considerable advantage to measure these low-resistive reactances as admittances rather than as impedances, as reasonably large readings free from harmonic trouble can be obtained.

Most commercial oscilloscopes are arranged with time constants in the amplifiers, etc.,

enabling them to amplify down to very low frequencies.

In consequence they do not like switching operations. The spot is apt to be thrown off the scale, and it takes some time for it to regain its new position.

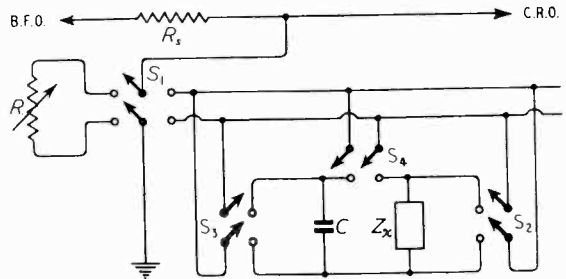


Fig. 6. Practical arrangement of the apparatus;  $R$  and  $C$  are resistance and capacitance boxes respectively and  $Z_x$  is the unknown impedance.

This can be corrected by reducing the valve coupling capacitors in the oscilloscopes used to much smaller values, not sufficiently small, however, to interfere with the amplification at the frequencies being used.

In the average laboratory there is a lot of mush liable to be picked up when large amplification is used, particularly when capacitors are being measured. This mush is mostly of fairly low frequency and tends to give blurred reading edges or points.

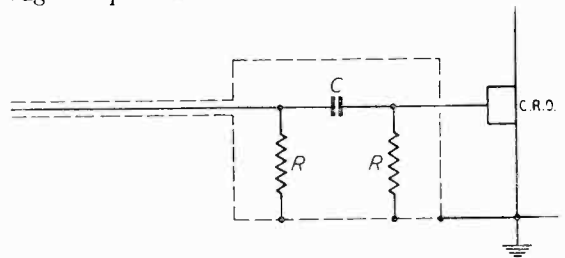


Fig. 7. This diagram shows a method of reducing mush; it consists of the insertion of a screened filter in the connection to the oscilloscope. For cut-off below 1,000 c/s, suitable values are  $R = 100 \text{ k}\Omega$  and  $C = 0.002 \text{ }\mu\text{F}$ .

This is best countered by inserting a small resistive high-pass filter, cutting off below, say, 1,000 c/s fitted in a small earthed shielding box on to the c.r.o. amplifier terminal, as shown in Fig 7.

### Frequency Stability

For particular work where great accuracy of frequency measurement is necessary, a frequency checking method based on multiples of a standard 1,000 c/s fork can be used, the chief point being to assure that there is no frequency drift of the b.f.o. during a series of measurements.

## Components

### Switches

For switching arrangements four telephone key-type switches were used in the original apparatus and fitted on a panel with other necessary terminals for connecting the b.f.o., c.r.o., unknown, resistance box and capacitance box. Some watch has to be kept on these telephone key switches to see that contacts are good, but a dirty switch will at once show up during a measurement.

One or two switching arrangements were made up with a better type of switch of the low-capacitance type. Ordinary porcelain-based, double-pole, double- and single-throw switches fitted to a breadboard are quite satisfactory, but possibly not so neat in appearance.

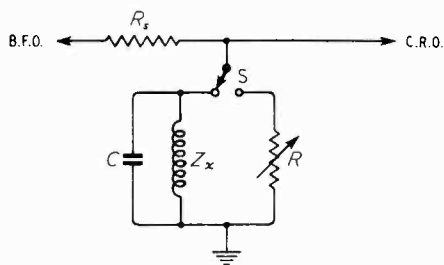


Fig. 8. Connection for admittance determination.

### Resistance and Capacitance Boxes

Any well-known resistance box of the non-inductive type will do, but probably it would be advisable to check whether the inductance is really negligible, and this can be done by comparing its action against resistances of the rod type over a wide range of frequency.

The mica capacitors used were made up in a decade form. They were all tested to see if they were up to standard, but their exact value was not noted as this is determined when the measurements are being made.

Of course such a box is far cheaper than a proper decade box with its accurate capacitors and can usually be made up with stock capacitors from the laboratory. Snap switches of a miniature lighting type enable each capacitor to be thrown in at will.

For general use three decades were used, viz., 0.5, 0.2, 0.2, 0.1  $\mu\text{F}$ , 0.05, 0.02, 0.02, 0.01  $\mu\text{F}$  and 0.005, 0.002, 0.002, 0.001  $\mu\text{F}$ .

A good mica capacitor has extremely small loss, but if one is suspected for loss it can be compared against one or two others of about the same value using the b.f.o. as a source of variable a.c. and resonating them with a high- $Q$  coil.

## Applications

The original apparatus was mainly used for determining the behaviour of ferro-magnetic cores—particularly when the latter exhibit magnetostriction effects. In these cases it is sometimes desired to take impedance measurements at much larger flux densities than would be given by the swamping resistance constant-current method, as the latter would become very uneconomical. It was found that satisfactory results could easily be obtained by replacing the swamping resistance by a thermal meter. Actually a large power amplifier was inserted after the b.f.o. and readings taken with powers up to 100 watts.

If the apparatus is maintained in an operating condition it will be found to be extremely useful for determining quickly, resistance values, capacitor values, resonance curves, network impedances, line impedances and for certain valve impedances which are of comparatively low value.

### Admittance Measurement

The method obviously lends itself to the direct measurement of admittance, a little calculation being necessary to obtain mhos from ohms after each balance.

In the admittance measurement the added capacitor  $C$  should be placed in parallel with the unknown. The diagram for this is shown in Fig. 8 and the graph for the determination of the admittance vector is shown in Fig. 9 where the distance  $OA$  represents the admittance of the added capacitor.

The final vector  $OV$  measured in mhos, if arithmetically inverted, gives of course the impedance, the vector angle remaining the same value but negative.

It will be noted that the switching system of Fig. 6 permits the paralleling of the capacitor with the unknown by throwing  $S_2$  and  $S_3$  together ready for the balancing operation.

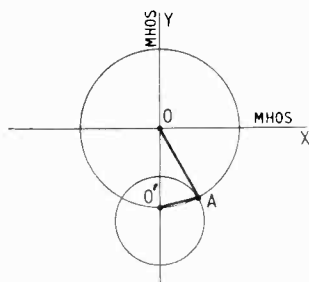


Fig. 9. Diagram for admittance determination.

The admittance measurement is very useful when the resistive component of the impedance is small (i.e., the  $Q$  value is high) because in this case when a series additional capacitor is used and the second balance obtained readings are rather small, amplification has to be large and harmonics tend to show up.

The admittance values, being balanced by a large resistance, do not suffer from these troubles.

### Errors and Defects

In attempting to maintain constant current by a swamping resistance unless the ratio of the resistance to the unknown is infinite some error will usually be introduced when the unknown is reactive for the total current passing is then slightly larger than if the unknown were resistive.

Roughly, one can say that if the swamping resistance is ten times the unknown then there will be a possible 10 per cent error, and if the swamping resistance is 100 times the unknown, there will be a 1 per cent possible error. These lie well within the order of other errors.

Of course the error does not occur if the unknown is only resistive.

The usual practice is to vary the swamping resistance according to the job being done, taking a reasonable balance between the error likely to be introduced by too low a resistance and the fact that it is not quite so nice if the amplification has to be too large.

Impedances below 2 or 3 ohms are troublesome to measure owing to the various lead impedances, and impedances over 500 ohms will require swamping resistances of sufficiently large value to give capacitance errors at the higher frequencies.

The usual practice with the c.r.o. is to operate it with a time base working—one which does not show a distinct waveform being preferable unless it is desired to watch the waveform. This will allow a top and bottom edge to be set between horizontal lines marked on the tube—if a spot only were used there would be a tendency to burn the tube.

## PHYSICAL SOCIETY'S EXHIBITION

THE 34th annual exhibition of scientific instruments and apparatus organized by the Physical Society was held at Imperial College, London, from 31st March to 5th April. The attendance was at least as large as ever, but complaints of overcrowding last year appeared to have been heeded, for there was a marked improvement, obtained by extending the exhibition both in space and time. Although there was again no official division into Trade and Research sections, the group of stands occupied by the considerable number of establishments now included in the Department of Scientific and Industrial Research and the Ministry of Supply comprised in effect a distinct research section. Except for a few of the larger firms, the commercial exhibitors confined their items mainly to production or prototype models.

### Materials

A material of increasing importance in the radio and electronic industry is the element germanium, of which a number of applications were shown. As a result of co-operation between the G.E.C. Research Laboratories and Johnson, Matthey, processes have been established for extracting it from flue dusts. Specimens of the dust, of the oxide and of the metal, were shown on the G.E.C. stand. Another element now being produced in this country is tantalum, which was featured by Murex, along with tungsten and molybdenum.

Progress in permanent-magnet alloys continues; an outstanding development, which was shown by the Permanent Magnet Association, is Alcomax having orientated columnar crystal growth, with  $BH_{max}$  as high as  $8 \times 10^6$  gauss-oersteds. For magnets in which anisotropic materials such as this are unsuitable, there is Hynico II isotropic alloy;  $BH_{max}$   $1.6 \times 10^6$ . Some examples were shown of the remarkable reduction in size, weight and cost of magnets for meters, loudspeakers, television focusing, etc.

Another magnetic material with which progress has been made since last year is the non-conductive ferrite group. Mullard demonstrated Ferroxcube IV and V; the advantages of IV over III are the higher a.c. resistivity and the lower permittivity, enabling it to be used advantageously at frequencies as high as 100 Mc/s. Ferroxcube V has been developed for its higher saturation magnetization (4500–5000 gauss). The absence of eddy-current loss renders these materials particularly valuable for low-loss high-frequency magnetic cores, but there are many other applications. For example, the Telecommunications Research Establishment demonstrated the use of their rapid loss of magnetic properties at the Curie point for thermostatic control. Caslam, the core material with a laminated structure shown last year by Plessey, has been further developed, mainly in the direction of improving its characteristics for the higher frequencies.

Progress was also to be noted in the group of ceramic materials with extremely high permittivity. While for some purposes the variability of characteristics with temperature and the appreciable loss angle render them inapplicable, these properties are no disqualification for by-pass capacitors, in which the criterion is the minimum  $\kappa$  over the working range of temperature. This was illustrated on the Mullard stand with reference to the new material K.3000, the name implying that the permittivity is greater than 3000 over the range 10°C to 70°C. The possibilities of this material for thermostatic control were demonstrated by T.R.E. alongside the Ferroxcube method just mentioned. The characteristics give a practically linear reactance/temperature relationship over a range of at least 100°C.

Plessey showed conductive ceramics made up as resistors for values to 0.1 MΩ. By varying the composition the temperature coefficient can be made positive, negative, or zero; and the properties do not alter appreciably up to 400°C.

Johnson, Matthey's stand was, as usual, devoted mainly to alloys and other special materials. High-accuracy low-loss waveguide tubing is now available, with silver lining if required. This firm can also do circuit printing in silver paint fired on to glass or ceramic panels. Examples were also shown of silvered-mica plates for the manufacture of high-quality stable capacitors. An interesting feature is a 'grid' plate designed to enable the capacitance to be adjusted precisely to the desired value.

A remarkable demonstration of the piezo-electric properties of quartz was staged by Standard Telephones, in which a quartz sphere about the size of a golf ball was made to run continually up and down a pair of horizontal rails without visible motive power. The remarkable feature was that in doing so the ball did not rotate!

## Components

The Standard Telephones exhibits also included sealed capacitors, illustrating successful manufacturing techniques, and demonstrations of thermistors. Among the increasing applications of thermistors is their use to protect the heaters of c.r. tubes in a.c./d.c. television receivers from switching-on surges. Among the components shown by Plessey were additions to their Breeze range of cable connectors and to their microwave accessories.

An ever-present need is a selection of instrument switches having good characteristics at a reasonable price, and W. G. Pye & Co. seem to have supplied it with their new A.218 series. These switches are available up to poles  $\times$  ways = 12 per unit; the brush-to-contact resistance is given as  $0.001\Omega$  for beryllium-copper and  $0.0002\Omega$  for copper, and the thermal potentials less than  $1\mu\text{V}$ . The former have been tested up to 100,000 operations without deterioration.

To avoid wearing and displacement of elements in the usual type of sine/cosine potentiometers, Elliott Bros. have introduced a new design in which simple replaceable elements are used and the law is obtained mechanically by a hypocycloid gear.

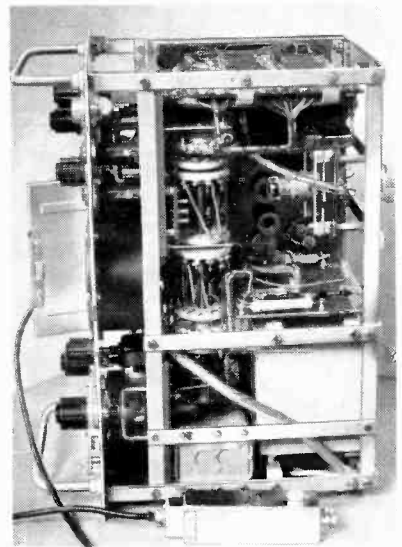
*B.T.H. magnetic field strength meter operating by the Hall effect in germanium.*



## Meters

Although there was an excellent display of straightforward types of meters, there seems to be little scope

for technical novelty in this field. Worth mentioning because of the scarcity of voltmeters suitable for present-day television c.r. tubes is the Everett Edgcombe three-range portable electrostatic instrument reading up to 10 kV. The upper ranges are obtained by high-resistance multipliers, and the maximum current drain is about  $10\mu\text{A}$ .



*Interior of the AVO test meter, type W tropical, showing the probe.*

Magnetic measurement is another sphere in which availability of instruments has lagged behind requirements; and because of the very wide use now made of magnets the magnetic field strength meter shown by B.T.H. is particularly interesting. It employs the Hall effect in a minute piece of germanium mounted in a probe that can be used to explore quite small gaps. The probe is connected to a portable microammeter which is direct reading up to 25 kilogauss, in three ranges. This use of the Hall effect in germanium was also demonstrated by the G.E.C. Research Laboratories. Instruments for measurements of magnetic flux and permeability were shown by Metrovic.

A signal output power meter by Marconi Instruments was notable for the exceptionally wide power range— $20\mu\text{W}$  to  $10\text{W}$ . It includes also some interesting new techniques in the methods of covering the usual 2.5–20,000 $\Omega$  impedance range over a frequency range of 500:1.

New types of valve voltmeter were not quite so numerous as in recent years; but there was a millivoltmeter by Airmec, using an amplifier with negative feedback to give ranges 0–10–100–1000 mV from 30 c/s to 5 Mc/s. Another was the AVO precision valve voltmeter, combining a wide range of a.c. and d.c. measurement with B.S.1 accuracy. The basis is a double-triode amplifier, with active and compensating diodes for a.c. An example of the same class of instrument was shown by Electronic Instruments. The AVO type W wide-range electronic test meter was displayed in tropical form.

## Amplifiers

Closely connected with the meter category is the AVO Television Signal-Strength Adapter, which aroused considerable interest owing to the increasing rate of television receiver installation and the great value of having some idea of the signal strength available on site. This instrument consists of an amplifier made up in the well-known AVO format and giving a gain of 20,000 over one of the television channels. The aerial is plugged in, and the signal strength is read in microvolts on an electronic testmeter or other valve voltmeter.

Other types of amplifier on view exemplified progress in frequency range at both ends of the scale, and high gain with stability, especially at zero frequency. The zero and very low frequency types have been developed for physiological applications, strain-gauge recording, and other special uses, and can be classified into those using direct couplings with stabilization, and those in which the signal is modulated in order to raise the frequency. Examples of the former class were shown by Pye and Southern Instruments, and of the latter by Tinsley and Sunvic. Extension into the high frequencies is chiefly in the interests of oscillography; high-gain amplifiers covering 0-10 Mc/s were prominent among the Nagard exhibits, both separate and incorporated into oscilloscopes. At the other extreme was an amplifier shown by T.R.E., using a twin-T RC network, with a bandwidth of 1 c/s at 1000 c/s, designed to select a signal from a noisy background. The same type of network was used by Tinsley in a bridge amplifier tunable over the exceptionally wide range of 16 c/s to 160 kc/s.

A simple type of self-rectifying amplifier is the essence of a compact electronic relay by Labgear, controlling up to 1 kW with 20 $\mu$ A input.

An amplifier for demonstrating a.f. technique in schools, etc., was among the 'custom-built' units shown by A. E. Cawkell. Magnetic amplifiers were to be seen in various applications. In a demonstration by Electro Methods, a multi-stage magnetic amplifier was coupled to an integrating motor, the effective starting power being 10<sup>-3</sup> $\mu$ W.

## Oscillators and Signal Generators

A number of firms showed new or improved a.f. oscillators, usually RC types, covering 20-20,000 c/s in three decades (Dawe, Pye, and Muirhead), but occasionally with a wider range (15-50,000 c/s, Advance Components; and 10-100,000 c/s, Cinema-Television). The trend is in favour of resistance-variation and thermistor amplitude-control, and improvements are chiefly in the direction of purer waveform and more constant amplitude. A v.f. oscillator (7 kc/s to 8 Mc/s) by Wayne Kerr covers the band in 6 ranges of 'straight' LC tuning, with total harmonic distortion less than 0.2% and amplitude variation not exceeding 0.1 db.

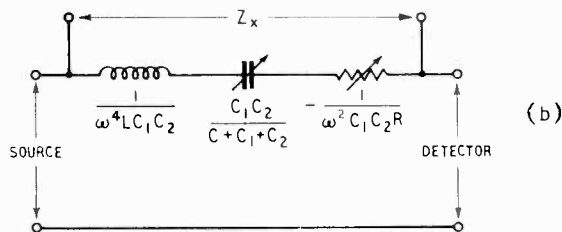
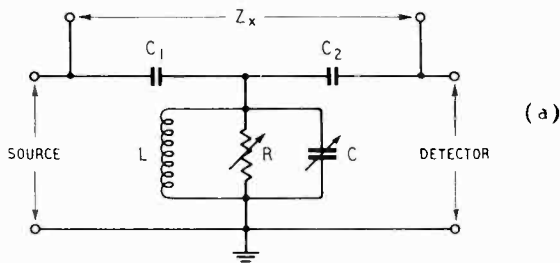
In the r.f. field, there were examples of frequency modulation and pulse modulation. The f.m. signal generator E.7572 by Mullard is intended for servicing receivers in the 80-104 Mc/s band; both sinusoidal and saw-tooth modulation are provided. In a new signal generator (TF.995) by Marconi Instruments, both f.m. and a.m. are available over a carrier-frequency range of 13.5-216 Mc/s; a crystal calibrator is built in. The same firm was showing a 8-14 cm oscillator employing

a reflex klystron with non-contact piston tuning. A coaxial-line velocity-modulated oscillator of the single-transit type shown by Standard Telephones was arranged for f.m. with a high degree of linearity (third harmonic, -65 db, for 1.75 Mc/s deviation) for microwave links. Square-wave and pulse technique was exemplified in a 600-1,215 Mc/s signal generator on the T.R.E. stand.

The great value for testing purposes of a source of square waves and pulses with a very short time of rise was demonstrated by Cinema-Television with their generator in which the time of rise is of the order of 0.015 $\mu$ sec. Pulse widths of 0.05-0.3 $\mu$ sec are available. Incidentally, a very special oscilloscope was needed to show the sharpness of waveform. Circuits for the generation of pulses as brief as 0.01 $\mu$ sec were shown by G.E.C.

## Bridges and Standards

An addition to the Wayne Kerr series of bridges was an experimental a.f. model in which the interesting feature is the replacement of variable C and R standards with fixed standards connected to decade variable-ratio transformers. A transformer error of only 0.001% up to 1 kc/s is claimed for a unit covering five decades. Besides reducing the cost of highly accurate standards, this system reduces residual errors by enabling the impedance of the bridge to be extremely low. The present trend towards inductively-coupled ratio arms or other devices to bring both source and detector to earth potential so

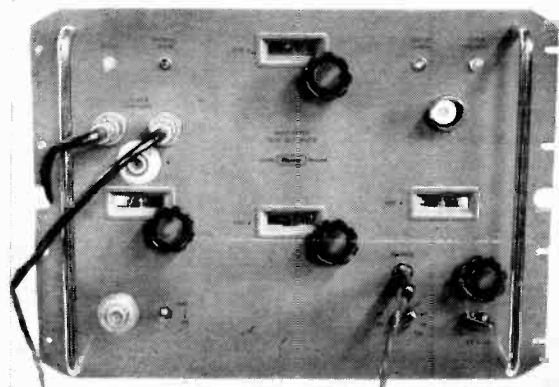


$$R_x = \frac{1}{\omega^2 C_1 C_2 R} \quad X_x = \frac{1}{\omega C_1 C_2} \left( C + C_1 + C_2 - \frac{1}{\omega^2 L} \right)$$

Circuit of 50-100 Mc/s T bridge (a) and its equivalent network (b) shown by S.R.D.E.

that components can be measured *in situ* regardless of the impedance from their terminals to earth was seen in two bridges by Cinema-Television; one for C and R and the other for L and M, both covering very wide ranges, with convenience in use and freedom from stray effects even when measuring small fractions of 1 pF or of 1 $\mu$ H.

The accompanying circuit diagram shows, at (a), the form of a 50-100-Mc/s T bridge network demonstrated by S.R.D.E. Its electrical equivalent is as at (b), from which it can be seen that the standards provide negative resistance and both positive and negative reactance, enabling an unknown impedance to be balanced out and its resistance and reactance determined from the relationships stated on the diagram.



*Plessey wavemeter covering 15-10,000 Mc/s.*

Among the various standards may be mentioned: push-button v.h.f. attenuators by Standard Telephones covering 0-9 db in 1-db steps or 0-90 db in 10-db steps up to 100 Mc/s; resistance standards by Tinsley with an accuracy of 1 in  $10^9$ ; an extension of the Muirhead universal series to include highly-stable units of 2 M $\Omega$  each; small standard Weston cells by Muirhead and Doran (the latter operable in any position); and quartz frequency standards as low as 400 c/s by Salford Electrical Instruments. Measurement of exceptionally high frequencies is provided for with an accuracy of 1 in  $10^9$  in the Plessey Test Set 272 covering 15-10,000 Mc/s, by reference to a calibrated butterfly-circuit oscillator of 400-800 Mc/s, in conjunction with other oscillators and a 100-ke/s crystal. A G.E.C. demonstration showed how still higher frequencies, in the 20-30 kMc/s band, can be measured by reference to molecular resonance of ammonia, contained in a coiled waveguide.

## Valves and Cathode-Ray Tubes

Important new types of valves were conspicuously absent, unless one includes transistors (germanium-crystal triodes). These have been considerably developed, and the production difficulties and fragility associated with critically-spaced 'cat-whiskers' have been largely overcome. In the design shown by G.E.C. they are replaced by two plates separated by a known and accurately controlled spacing. Applications on view included a miniature 3-stage amplifier with a gain of 66 db.

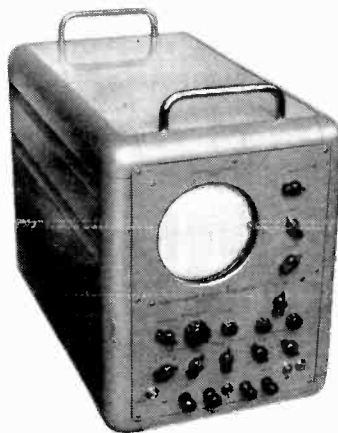
The E.M.I. Multiplier Photo-tube, which is an 11-stage electron multiplier with a photo-electric cathode, having an overall multiplication of about  $10^7$ , was shown in two improved forms. It is used in television film-scanning equipment and still more widely in nuclear research as a scintillation detector.

The cathode-ray tubes shown by 20th Century Electronics were designed as precision instruments.

They have flat screens and the electrodes and deflector plates are accurately aligned in a rigid mounting. The double-beam type has common X plates but separate Y plates and guns, and is therefore free from inter-modulation.

## Oscilloscopes

As mentioned in connection with amplifiers, the trend is towards wider ranges of frequency, and it is now normal for instruments to include z.f. amplification. An outstanding example was shown by Mullard, with identical X and Y amplifiers effective from 0-20 Mc/s. The Nagard instrument can be made up to a variety of specifications, including the amplifiers already referred to, and is designed for accurate measurement of time, frequency, and voltage. The power unit is separate. Another oscilloscope with z.f. amplifiers was that shown by Industrial Electronics, in which the time-base frequency can be made as low as a few cycles per minute. T.R.E. exhibited a large console type of laboratory oscilloscope with 12-inch tube, designed to give the utmost accuracy of measurement. Equipment on the Avimo stand was devoted to oscillography, as distinct from oscilloscopy, and included high-speed recording cameras. In a specialized type of instrument shown by the Armament Research Establishment, for the accurate timing of events, the display took the form of a crystal-controlled spiral, giving a 50- $\mu$ sec base on which events at intervals of from 0.2  $\mu$ sec can be recorded with an accuracy of 0.02%.



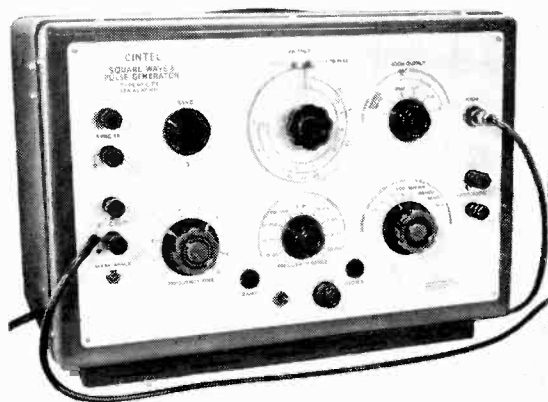
*Industrial Electronics audio-frequency response-curve tracer.*

## Special Apparatus

Some of the instruments in this category could be regarded as oscilloscopes plus; for example, the Industrial Electronics portable a.f. curve tracer, which consists of a b.f. oscillator with automatic frequency sweep, in conjunction with a c.r. oscilloscope. The Y deflection is obtained from the output of the apparatus under test, and the X deflection is provided by a RC discriminating circuit giving a voltage proportional to the logarithm of the oscillator frequency. The Standard Telephones cable-testing equipment employs radar technique with a c.r. tube display, to detect any non-

uniformity of impedance such as would be caused by a fault, and to indicate its distance from the point of test. Other tests, such as loss measurement and velocity ratio, can be easily performed with the same equipment.

If a prize were to be awarded for the instrument which would keep visiting radio engineers instructively entertained for the longest period by manipulating the knobs, it would almost certainly have gone last year to the Cinema-Television valve tester (seen now in production



*Cinetel pulse generator with a pulse rise-time of 0.015 $\mu$ sec.*

form). This year it would no doubt have been earned by another c.r. instrument—the T.M.C. electronic analogue computer for directional aerial arrays. This is provided with current, phase, and spatial angle knobs for each of three aerial dipoles; and by turning these the corresponding radiation pattern of the array can be seen on the screen. As an alternative to laborious trial-and-error computations, or field-strength measurements, there is very much to be said for this scheme, by which the result of any combination of parameters can be seen in a few seconds.

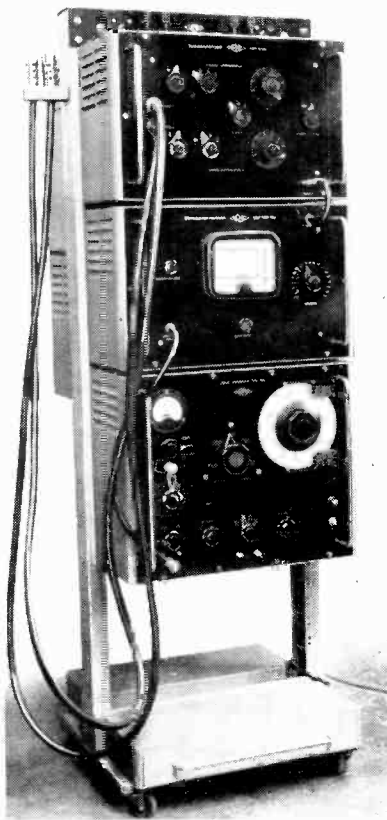
In view of the importance of the Nyquist criterion in modern amplifier design, the phase-measuring equipment made by Airnec for the G.P.O. Research Department is of great interest. Its frequency range is 50 kc/s to 20 Mc/s, and accuracy of measurement  $\pm 3\%$ . Contact with the two points between which the phase angle is to be measured is made by two probes having an input capacitance of 6 pF; and the range of input level is 66–27 db below 1 V.

In addition to those already mentioned, new Marconi Instruments items on show included a 8–11-cm oscillator, a spectrum analyser for testing magnetrons in the same band, a 3-cm waveguide test bench, a noise-factor meter incorporating a calibrated noise diode, a receiver tester improved by the addition of a 1-db step attenuator and a mechanical frequency-increment control, and an a.f. change-of-level recorder. An instrument of the last-named type was also shown by Dawe; and a spectrum analyser for the 3-cm waveband by Elliott Bros. Comprehensive 3-cm and 10-cm waveguide test equipment was among the B.T.H. display.

Measurement of noise factor at 10,000 Mc/s (of travelling-wave amplifier tubes) was demonstrated by Mullard with a waveguide set-up in which a signal

from a klystron could be passed either direct or via the amplifier. Another Mullard demonstration showed measurement of valve input damping in the range 10–150 Mc/s. It was based on the voltage developed across a tuned input circuit. A direct-reading f.m. deviation meter was shown by the Signals Research & Development Establishment, for measuring deviations up to 500 kc/s at frequencies up to 120 kc/s, on carriers of 20–100 Mc/s, to an accuracy better than 2%.

In acoustical measurements, one of the difficulties has been that of completely suppressing reflections at the lowest frequencies. The solution adopted at the National Physical Laboratory was illustrated by a model of a duct, reminiscent of a large-scale waveguide, with one end containing the source of sound and the other terminated by absorbing wedges. The microphone, located about midway, is subjected to a plane progressive wave, disturbing effects being reduced to the order of 1% in the range 25–450 c/s.

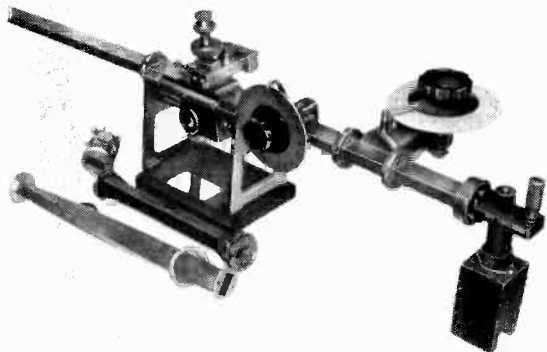


*Airnec phase-measuring equipment covering 50 kc/s to 20 Mc/s.*

## Power Supplies

Many exhibits illustrated the interest in stabilization of power supplies to meet increasingly exacting requirements. For smoothing out a.c. mains voltage variation, the improved Zenith automatic voltage regulator provides for up to 20 kVA single-phase. It has a motor-

driven regulator controlled by a non-linear a.c. resistance bridge with two tungsten-lamp arms. The Tinsley a.c. stabilizer, to Dr. Patchett's design, deals more precisely with smaller amounts of power (0.5 kVA), giving a short-



*Marconi Instruments standing-wave detector.*

term stability of 1 in 5,000, and is compensated for temperature variations. An example of the well-known negative-feedback type of voltage stabilization applied to rectified and smoothed a.c. was shown by A. E. Cawkell, with heater stabilization of the valves in order to give a much closer control than is possible without. Current stabilization, other than by simple barretter lamps, has not had so much attention, but a method demonstrated by the British Scientific Instrument Research Association made use of a saturated transductor to stabilize heater current at any pre-set value between 0.2 and 0.6 A r.m.s.

The Elimiac l.t. power unit by Labgear is not stabilized, but provides 0-15 V d.c. with extremely small ripple (0.1% at 5 A and 0.01% at 2 A), in addition to 0-20 V 10 A a.c.

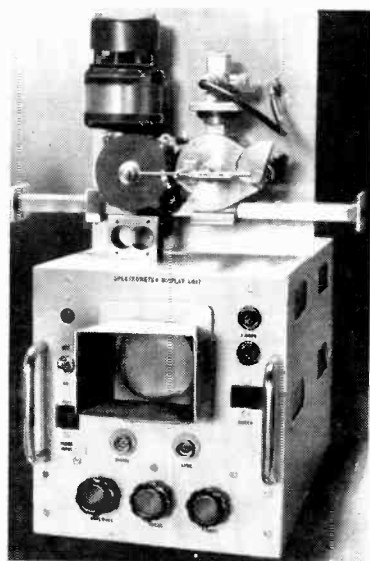
## Research

A number of exhibits of the research establishments have already been mentioned, and many others fall outside the scope of this journal. An interesting joint display by T. R. E. and the Meteorological Office explained the working of the most recent form of balloon-borne meteorology—the radar sonde. By its means a single ground station automatically keeps a continuous record of the height of the balloon and (from its motion) wind speed and direction, as well as receiving the atmospheric data transmitted by it—pressure, temperature and humidity. The ground station sends pulses on a wavelength of 2 metres, which are returned by a transponder

in the balloon on 10 cm. The distance is determined in the usual way by the transit time, and the bearing and elevation from an auto-follow aerial system; the information is fed into a computer. The data registered on the balloon-borne instruments are conveyed by pulses following the range pulse.

Peculiarities of radio propagation over a land-and-sea path were demonstrated by Marconi's Wireless Telegraph Co. with a small-scale model, using a fixed directional 3-cm sender and a receiver mounted on a small trolley. Sea was simulated by a metal sheet and land by metal covered with paxolin.

A resistor network for solving partial differential equations, such as Laplace's and Poisson's, to high accuracy (1 part in  $10^3$  to  $10^4$ ) was shown by the A.E.I. Research Laboratory applied to the calculation of the electric-field pattern in an electron lens.



*Elliot X-band spectrum analyser.*

A demonstration by B.T.H. showed a new system of pulsing high-power 3-cm magnetrons without the use of any valves or discharge devices. The circuit consisted of a chain of saturated reactors (named Pulsactors) utilizing the extremely sharp magnetization knee of core materials such as H.C.R. metal to provide the pulse-switching action. The system has the advantages of long life and stability.

# CORRESPONDENCE

Letters to the Editor on technical subjects are always welcome. In publishing such communications the Editors do not necessarily endorse any technical or general statements which they may contain.

## Electron Transit Time

SIR.—In your February issue there is an article by Chatterjee and Sreekantan on the effects of electron transit time on negative-grid oscillators. In that article the authors use certain formulae of mine but they do not take sufficient account of the assumptions made in deriving the formulae. There are several aspects of their paper which are open to question but I would particularly refer to their use of the equation\*

$$\eta_1 - \eta_2 = \frac{\sqrt{2} \hat{e}_a}{\pi E_a} \omega^2 \tau^2$$

which is the same as equation (3) in their paper. This formula gives the difference between the low-frequency efficiency,  $\eta_1$ , and the efficiency,  $\eta_2$ , at a frequency corresponding to a transit angle of  $\omega\tau$ . In deriving the formula it was assumed that the only effect of the electron-transit time was to introduce a phase delay in the anode current pulse, so that the maximum current did not occur at minimum anode voltage. This assumption was made originally in an attempt to establish a connection between the efficiency and the onset of transit-time effects. In view of the simplifying assumptions made in deriving the above formula, its application to much higher frequencies is unjustifiable. When the transit time is an appreciable fraction of the alternating period, the shape of the anode-current pulse will differ considerably from its shape at low frequencies. Again, the kinetic energy of the electrons at the anode will not correspond to the potential of the anode at the instant of arrival. In view of these and other assumptions, it is not surprising that Chatterjee and Sreekantan found very little correlation between the observed and calculated values of their  $\lambda_2$ .

Cambuslang,  
Glasgow.

M. R. GAVIN

\* *Wireless Engineer*, June 1939, Vol. 16, p. 287.

## Background Noise in Photomultipliers

SIR.—It is a fairly common observation that incident radiation causes the background noise to increase, beyond the level due to 'dark current' alone. This is expressed by the noise equation (1) which has appeared elsewhere<sup>1</sup>. It seems worthwhile to present this equation in a more explicit form, since a number of important conclusions are to be derived from it.

The mean square value of shot-noise current, in a bandwidth range  $B$  cycles per sec. is

$$\overline{i_n^2} = 2e(\bar{i} + i_p)B \quad \dots \quad (1)$$

where  $\bar{i}$ ,  $i_p$  are the respective values of 'dark current' and emission current from the photocathode.

Suppose that the signal current (i.e.,  $i_s$ ) is to be  $s$  times the r.m.s. amplitude of the noise current, then

$$i_s^2/s^2 = 2e(\bar{i} + i_p)B \quad \dots \quad (2)$$

so that

$$i_p^2 - 2es^2B i_p - 2es^2B \bar{i} = 0 \quad \dots \quad (3)$$

and therefore

$$i_p \text{ must equal } es^2B \left[ 1 + \sqrt{1 + \frac{2\bar{i}}{es^2B}} \right] \quad \dots \quad (4)$$

Consequently for a given signal-to-noise ratio the required value of  $i_p$  is not much affected by  $\bar{i}$ , provided that  $\bar{i}$  falls below, say,  $\left(\frac{es^2B}{2}\right)$ .

For wideband amplifiers  $\bar{i}$  need not be so small as for a narrow band. Further, it should be noted that effects of refrigeration cannot be assessed without a knowledge of the values of  $s$  and  $B$  which are needed for any particular application.

New Barnet, Herts.

S. RODDA

<sup>1</sup> Engstrom, R. W., *J. opt. Soc. Amer.*, June 1947. (Eqn. 3).

## Change of Mutual Conductance with Frequency

SIR.—In the March 1950 issue there is a letter by Eisenstein reporting on the results of a study of the decay of anode current passed by a pentode when a square voltage pulse is applied to the grid. The results are explained by the development of a homogeneous interface compound sandwiched between the coating and the base metal of the cathode. Eisenstein states that this, rather than the inhomogeneous poor contact hypothesis offered by Raudorf, is the correct explanation of the change of  $g_m$  observed by Raudorf<sup>1</sup>.

As a matter of fact the frequency dependence of  $g_m$  was first blamed on the development of an interface compound when, some ten years ago, the change of mutual conductance with frequency in the course of operation caused serious trouble in communication receivers of the R.P.Z. (Reichspost Zentralamt). It turned out, however, that this was not justified. The geometrical structure of the base metal proved to have a decisive effect on the development of the cathode impedance, in comparison with which the influence of an interface compound was of minor importance. The improved behaviour of flat cathodes was confirmed by measurements on a range of valves of German and foreign make. It would be interesting to hear whether Eisenstein investigated the influence of the curvature of the core surface on the development of the cathode impedance before writing his letter.

Department of Physics,  
University of Birmingham.

W. RAUDORF

<sup>1</sup> W. Raudorf, *Wireless Engineer*, October 1949

## Non-Linear Distortion in a Cowan Modulator

SIR.—The main non-linear distortion product  $f_3 + 3f_s$  in balanced rectifier modulators was calculated in previous letters<sup>1,2</sup>. Although the theoretical distortion agrees with published experimental results<sup>3</sup> for the ring modulator, there is an apparent numerical discrepancy between the predicted distortion and results obtained by Tucker and Jeynes<sup>4</sup> for the Cowan modulator.

The latter experiments are difficult to interpret because the practical conditions do not permit a simple approximate calculation. Using the notation of reference (2), it is apparent that the approximate formula (18) deduced there from (16) is only correct when both  $cV_s/V_c$  and  $bV_s/V_c$  are small compared to 1. Now, in the experiment,  $bV_s/V_c$  has the constant value 0.43 and  $cV_s/V_c$  is equal to 1 for a c.s.r. (carrier source resistance) of 100 ohms, so that a second overload occurs for smaller resistances. Thus, the conditions for the approximate formula (18) are not met and the comparison with a more rigorous expression derived from (16) would require lengthy calculations using elliptic integrals, because of the strong interaction between the two overload effects.

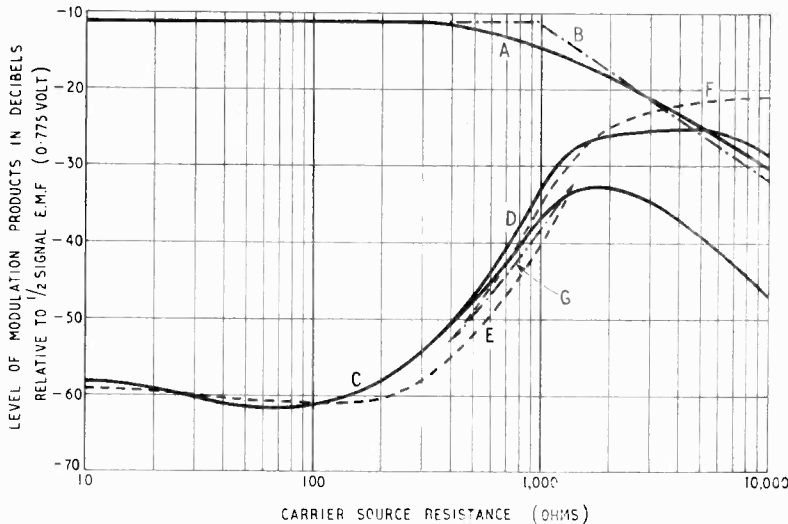
It seemed thus necessary to reproduce the experiments choosing more convenient practical conditions.

It appeared also preferable to adopt the carrier e.m.f., and not the positive peak p.d., as reference variable. In a Cowan modulator without a complementary rectifier in opposite connection the positive and negative peaks of the carrier p.d. are different and difficult to measure directly; also, the carrier p.d. contains a d.c. component which (unless adequate precautions are taken) is shunted by the d.c. resistance of the carrier source and this produces a complicated readjustment of the carrier voltages.

marked  $V_{11}$  and  $V_{13}$ ) for a signal to carrier ratio  $k$ , the distortion margin in our case will be

$$D(xV_s/E_c) \quad (3)$$

The results shown in the figure refer to a modulator composed of four KH1 copper-oxide rectifiers working between 600 ohms source and load. Both the signal and the carrier were in the voice-frequency range and varied to give 800 c/s for the modulation product being detected. The signal level (1/2 e.m.f.) was kept to 0 db relative to 1 mW in 600 ohms and the carrier e.m.f. was 10-db higher.



Bridge modulator in a 600-Ω circuit; carrier e.m.f. = 0.775 V + 10 db. Curve A, output level of  $f_c - f_s$ ; curve B, asymptotes crossing at the theoretical overload point (950-Ω); curve C, output level of  $f_c - 3f_s$ ; curve D, distortion margin calculated from  $C - A + 11$  db; curve E, theoretical value for C calculated by Equ. (2) holding for low c.s.r.; curve F, theoretical value for C calculated by Equ. (3) holding for high c.s.r.; curve G, common asymptote of E and F.

First, the main sideband level (curve A) was measured. The theoretical overload point corresponds to  $20 \log x = 10$  db; i.e., to a c.s.r. of  $300 \times 3.15 = 950$  ohms. This is marked B on the figure and the theoretical asymptote after overload has a negative slope of 20 db per decade of c.s.r.

The measured distortion  $V_{13}$  is curve C and the resulting distortion margin (except for the additive constant - 11 db) is curve D which coincides with C before overload. The margin calculated by equation (2) and using the known level - 11 db of  $V_{11}$  gives curve E, the theoretical value at zero c.s.r. being  $- 27.6 - 11 = 20 = 58.6$  db and curve F is the margin calculated by (3) and plotted downwards from the - 11-db line. Curve G is the common asymptote

$$V_{13}/V_{11} = (xV_s/E_c)^2/24$$

of both theoretical expressions and is a straight line of 40-db slope per decade of c.s.r., the intercept at the overload point being  $- 27.6 - 11 = - 38.6$  db.

The agreement between theory and experiment is satisfactory even for relatively high values of the c.s.r. As this corresponds to quite small positive peak carrier p.d. definitely in the non-linear part of rectifier characteristics, the experiment evidently shows that the exact rectifier law is not essential and that the distortion entirely depends on the effect of the signal voltage shifting, relatively to each other, the intervals of steep resistance change of the two pairs of rectifiers.

A similar statement holds for another kind of phenomenon. The presence of a spurious carrier  $f'_c$  modifies the simply periodic character of the rectangular switching function of frequency  $f_c$ . The difference between the switching functions with and without the spurious carrier is a wave composed of pulses of periodicity  $f_c$  modulated in width by  $f'_c$ . The harmonic analysis of such a wave gives an infinite number of components  $mf_c - f'_c$ , with  $m$  even or zero, and all having the same amplitude. An elementary calculation shows that, if the spurious carrier is  $A$  decibels below the main carrier, an infinite number of spurious modulation products  $mf_c - f'_c - f_s$  ( $m$  even or zero) will be present in the output at  $A + 6$  db below the main sideband level. This was checked experimentally with  $A = 30$  db using a Cowan modulator with a fifth opposing rectifier and, up to  $m = 12$ , the level drop of the spurious products was only 5 db.

Brussels, Belgium.

V. BELEVITCH.

#### REFERENCES

- 1 V. Belevitch, *Wireless Engineer*, May 1949, Vol. 26, p. 177.
- 2 V. Belevitch, *Wireless Engineer*, April 1950, Vol. 27, p. 130.
- 3 R. S. Caruthers, *Bell Syst. Tech. J.*, April 1939, p. 315, see fig. 3.
- 4 D. G. Tucker, E. Jeaynes, *Wireless Engineer*, Feb. 1950, Vol. 27, p. 66.

The basic equations of Ref. (2) were thus first rewritten in terms of the carrier e.m.f.  $E_c$ , which is directly measurable, and this produced a simplification in the formulae which no longer depend essentially on the rectifier ratio. It was, therefore, permissible to assume ideal rectifiers ( $g_0 = 0, g_s = \infty$ ) and the comparison with experiment involves no knowledge of numerical data on the rectifiers.

In terms of the instantaneous carrier e.m.f.  $e_c$ , equation (16) of ref. (2) becomes, for an ideal modulator,

$$v' = \frac{I}{2(1+x)} [F(e_c, v_s) + F(e_c, xv_s)] \quad (1)$$

where  $x = 2r/R$  is the ratio of the c.s.r. to the circuit source and load in parallel. By choosing for  $E_c$  in the experiment a constant value somewhat larger than  $V_s$ , the overload due to the first term of (1) will be avoided but, if the c.s.r. is gradually increased, an overload point due to the second term will occur for  $xV_s = E_c$ . Before this overload, the distortion ratio is given by

$$V_{13}/V_{11} = \frac{1}{24} (V_s/E_c)^2 (x^2 - x + 1) \quad (2)$$

and is minimum for  $x = 1/2$ . This is merely equation (18) of ref. (2) in the new notation. Near the overload point the rigorous expression involving elliptic integrals must be used for the second term in (1) but the contribution of the first term is negligible. The effect of the second term can be obtained graphically from the curves of reference (1). Denoting by  $D(k)$  the distortion margin read on these curves (interval between curves

### Gain of Aerial Systems

SIR,—Your contributor Mr. D. A. Bell suggests in Appendix II of his paper (*Wireless Engineer*, September 1949), and again in a letter (January 1950), that it is "theoretically possible for a limited spectral distribution of energy to produce a train of repeated pulses in which each pulse has any desired degree of narrowness."

This statement would be correct if the Fourier transform of an aperture distribution gave the polar diagram as a function of  $\theta$ , the angle with the normal to the aperture. In fact the variable in the Fourier transform is  $\sin \theta$ , which is therefore the exact analogy of time in the circuit problem. Now only that part of the Fourier transform in which  $|\sin \theta| \leq 1$  corresponds to the radiated polar diagram, so that obtaining an abnormally narrow diagram in this region corresponds to getting an abnormally sharp pulse in a given finite range of time. Outside this range of time the function will in general be very large indeed, as an examination of the examples given in our paper\* show.

Thus the circuit analogue of an anomalously narrow beam aerial is a pulse, obtained from a limited spectrum of frequencies, which during a finite interval of time, has a sharp peak, but which has broad 'humps' of very large amplitude outside the specified time interval.

Furthermore, if the aerial has a continuous aperture distribution, there will be one pulse only, but if the aperture distribution is composed of discrete sources spaced  $d$  apart, the polar diagram will be periodic in  $\sin \theta$  with period  $\lambda/d$ , so that the circuit analogue is a train of pulses. If  $\lambda/d > 2$  the period will extend beyond the  $|\sin \theta| \leq 1$  region, so that in the circuit analogue sharp pulses and large 'humps' will occur alternately; if  $\lambda/d < 2$  the period will not extend beyond the  $|\sin \theta| \leq 1$  region, and under these conditions anomalously high gain cannot be obtained.

Telecommunications  
Research Establishment.

P. M. WOODWARD.  
J. D. LAWSON.

\* *J. Instn. elect. Engrs*, 1948, Vol. 95, Pt. III, p. 363.

## NEW BOOKS

### The Theory and Design of Electron Beams

By J. R. PIERCE. Pp. 197 + xiii. D. Van Nostrand Co., Inc., 250 Fourth Avenue, New York 3, U.S.A. Price \$3.50.

Dr. Pierce, whose contributions to the design of microwave valves are well known, has written this short book to emphasize the aspects of electron optics which have to do with high-current low-voltage beams. These problems are of fundamental importance in valve design but most books on electron optics confine themselves to what might be termed geometric electron optics, in which the space-charge forces due to the electrons and ions in the beam are assumed to produce negligible effects. The theory thus developed applies well to such devices as electron microscopes and diffraction cameras, somewhat less well to modern cathode-ray tubes and hardly at all to the special types of valve using well-defined electron beams which are used at u.h.f.

The present book "represents an effort to collect together with reasonable orderliness the minimum amount of theoretical material necessary for a good understanding of electron flow and electron focusing in devices other than electron microscopes and image tubes." To this end rather more than half of the space is devoted to matter included in standard books on electron optics and only chapters 8, 9 and 10 deal with heavy-current flow. The basic theorems of electron optics are very clearly expounded, using the ordinary Newtonian forms of the equation of motion and the Lorentz force law. This treatment is much more suitable for beginners who have not specialized in geometrical optics than are the applications of least action, eiconals, etc., which are preferred particularly by German writers on the subject. Since in all practical heavy-current devices the geometrical aberrations are masked by space-charge effects it has not been necessary to deduce the elaborate theory of third-order errors. The treatment is made concrete by application to problems encountered in electron multipliers and beam-deflection tubes.

Turning now to the material dealing specifically with high currents, chapter 8 surveys the effects produced by thermal velocities. The main problem studied is the current density which is obtained when current from a cathode of given area and temperature is focused to a point or a line. In this case the beam is considered to have such a large cross-sectional area at all points, other than those in the immediate vicinity of the focus,

that space charge is unimportant and the factor determining the current density is the spread of thermal velocities which plays a part analogous to chromatic aberration. The results, originally due to D. B. Langmuir, are here deduced by the use of Liouville's theorem, as was done in an important paper by the author. The maximum current density given by these results represents an absolute maximum which can never be exceeded. In many cases, however, space-charge forces along the length of the beam are far from negligible and the current density is limited by space-charge considerations; it may be long, therefore, before the thermal limit is approached. This case is the subject of chapter 9, which includes both electrically and magnetically-controlled beams. A short section on the influence of positive ions is included.

Chapter 10 treats the special types of electron gun in which the electron flow is rectilinear. These guns were introduced by the author and are now known as 'Pierce' guns. The results of chapters 8 and 9 are then compared and it is shown how the angle of convergence, voltage and ratio of anode to cathode radius determine whether the thermal limit or the space-charge limit is operative.

The book is always clear and succinct, and the author has a very good knowledge of what is necessary and what can be neglected in this work. There are omissions, as is inevitable in a short pioneer monograph, and it is a pity that there should be no mention of the processes used for inserting a space-charge correction on trough plots or of the very general theory of beam focusing developed by Condon, Bunemann and Latter. Valve designers will welcome the book as a lucid exposition of problems whose solutions are scattered over an enormous literature and any research worker wishing to design an electron beam should consult it, if only to note Dr. Pierce's final remark that precious time may be lost by trying to do better than well enough. To Dr. Pierce belongs much of the credit for telling us how well we can ever do.

A. H. W. B.

### Recent Advances in Radio Receivers

By L. A. MOXON, B.Sc.(Eng.), A.M.I.E.E. Pp. 182 with 92 illustrations. Cambridge University Press, 200 Euston Road, London, N.W.1. Price 18s.

The author of this book is a leading authority on the subject of noise in radio receivers and we must not be surprised that almost exactly one-half of this book

is devoted to this aspect of receiver design. The design of i.f. amplifiers is also covered in detail while there is a separate, and valuable, chapter on the measurement of noise factor.

The remainder of the book deals with recent trends in communication and commercial receiver design but is so synoptic in treatment that it will only preach to the converted and it is in the earlier chapters on noise that the main value of the book resides. Although the matter on noise is exhaustive, as far as it goes, one might reasonably have expected a fuller treatment of the physics of the subject, for instance no mention is made of the work of N. R. Campbell and V. J. Francis. Again, although circuit noise is treated, in extenso, there is less than a paragraph on partition noise; the expression for cathode and partition noise is given without supporting argument and the desirability of a high  $I_m/I_K$  ratio is deduced on the strength of this quoted formula alone. There is, in fact, a lack of emphasis throughout the book which must inevitably reduce its value to the advanced student, as distinct from the practising design engineer.

The chapter on i.f. amplification covers, in considerable detail, the design of multiple stagger-tuned amplifiers but transient response and time-delay are treated in a somewhat cursory manner (we have the surprising situation that this important aspect of design gets little more space than image rejection in short-wave super-heterodynes).

Mathematical expositions have been avoided almost entirely, but the arguments are not necessarily easy to follow on that account. There is, for example, a marked absence of references to familiar concepts and expressions which should make a text flow freely; again it is not always clear whether a given expression should follow from the argument or whether it is being quoted from some other work.

Much of this lack of correlation can be attributed to the author's tendency to lift some of his material verbatim from his published articles; a very human frailty which rarely produces a really satisfactory result.

With the introduction of quantization methods of modulation, noise measurement assumes an added importance in the communications field and the chapter devoted to measurement can be unreservedly recommended to those who will be concerned with this subject.

The book is remarkably free from errors, as such, a careful check revealed only two, both fairly obvious and of minor importance.

As a whole, the book can be recommended because it brings under one cover much valuable information on receiver noise. One must, however, suggest that a more satisfying work could be produced, from the same pen, if the later miscellaneous chapters were excised in favour of an even more comprehensive statement on noise.

E. J.

### Die Maxwell'sche Theorie in veränderter Formulierung

By L. KNEISSLER. Pp. 51 and viii Springer-Verlag, Vienna.

This is a discussion of a suggested modification of Maxwell's theory. The author, who is a professor at Vienna, says that since the introduction of the Lorentz electron theory, Maxwell's theory has receded into the background. It was the difficulty of applying Maxwell's theory to magnetic fields in the presence of ferromagnetic materials that led the author to attempt a modification of the theory. The author states that his approach is that of a theoretical electrical engineer and not of a physicist. By eliminating magnetism and replacing it by the currents that produce it within the material, the author states that Maxwell's theory is brought into agreement with the electron theory in its macroscopic

form. The book is divided into four chapters dealing with, I, fundamental equations, II, dielectric material; III magnetic material, and IV, the general electromagnetic field. There is a short appendix dealing with the system of units employed. The author published articles on the subject in the *Archiv für Elektrotechnik* for 1940, 1941 and 1942, and the book is a development from these.

G. W. O. H.

### The M.K.S. System of Electrical and Magnetic Units

(Decisions taken by the International Electrotechnical Commission)

B.S. 1637: 1950. British Standards Institution, 24-28 Victoria Street, London, S.W.1. Price 2s.

It is stated in the Foreword to this 8-page memorandum that it does not express any opinions either for or against the system, but is issued with the object of putting on record in summarized form the decisions which have been arrived at internationally regarding the m.k.s. (Giorgi) system. At the Torquay meeting of the International Electrotechnical Commission in 1938 Professor Giorgi undertook to prepare a booklet, but owing to the war it did not materialize; hence the present memorandum. The question of rationalization is not discussed. A list is given of the principal units with definitions taken from Giorgi's memorandum, but modified where necessary to bring them into line with later decisions.

After defining the metre and kilogram the remark is made that "the metre and kilogram are the original units of the metric system; the centimetre has not a convenient size for everyday use, and nobody employs it in common life for measuring large distances or for deriving multiples and sub-multiples." This is not very convincing; one does not use the centimetre *nor the metre* for measuring large distances, and the gram is used for deriving multiples and sub-multiples, such as kilograms and milligrams. It has been suggested to us that the litre should have been mentioned, but although it is the most commonly used unit of volume in metric countries, it is not a unit of the m.k.s. system. It was also suggested that in giving the density of water as 1000, the temperature should have been specified, but it is not given as an accurate definition, but merely to indicate that the density is 1000 and not 1 in the m.k.s. system. The definition of the newton is very amusing. Instead of saying simply that it is the force that causes a mass of a kg to accelerate at 1 m/sec<sup>2</sup>, we are told that it is "the gravitational force on (or weight of) a kg mass in a place (about 20,000 km from the centre of the earth) where the acceleration due to gravity would be 1 m/sec<sup>2</sup>". The unit of work or energy is "the joule which equals the product of a newton into a metre"; this seems a strange use of the word 'product'.

The definition of the ampere as "the value of a constant current which when maintained in two parallel conductors . . ." would be more precise if the current were maintained in *each* of two parallel conductors. On page 6 there is a reference to "two carrying conductors"; we presume that the word 'current' has been accidentally omitted. It is stated that the inductance is defined as the ratio between an electromotive impulsion and a current; we feel sure that in this country it is more often defined as the ratio between an e.m.f. and the rate of change of a current.

The first four pages give a useful historical background to the present position, and useful extracts from Professor Giorgi's 1934 memorandum describing the system and discussing the subject of dimensions.

We feel, however, that the question which is worrying people at the moment is not c.g.s. or m.k.s.—that is generally regarded as settled—but rationalization or

non-rationalization. The pamphlet concludes with the decision arrived at in 1938 at Torquay " that the question of rationalization should be left over for the time being, as it did not appear sufficiently ripe yet for the adoption of final conclusions." That was twelve years ago.

G. W. O. H.

#### **The Electronic Engineering Master Index 1947-1948**

Pp. 339 + xiii. Electronics Research Publishing Co. Inc., 480 Canal Street, New York 13, U.S.A. Price \$19.50.

This index is to articles dealing with electronics and allied subjects which have appeared during 1947 and 1948 in the world's technical press. It includes also references to American, British and Canadian declassified documents covering some of the wartime research in electronics. American technical books are included and also patents.

The index is arranged under main subject headings and there is a cross index.

#### **The Radio Amateurs' Handbook, 1950, 27th Edition**

Pp. 615. The American Radio Relay League, West Hartford, Connecticut, U.S.A. Price \$2.50.

#### **Short-Wave Radio and the Ionosphere, 2nd Edition**

By T. W. BENNINGTON. Pp. 138 with 61 illustrations. Iliffe & Sons Ltd., Dorset House, Stamford Street, London, S.E.1. Price 10s. 6d.

This book presents the available information on the ionosphere in simple form so that it is usable by non-specialists in the subject. The approach is non-mathematical.

#### **Noise and Sound Transmission**

Report of the 1948 Summer Symposium of the Acoustics Group. Pp. 200 + iv. The Physical Society, 1 Lowther Gardens, Prince Consort Road, London, S.W.7. Price 17s. 6d.

#### **High Frequency Voltage Measurement**

By MYRON C. SELBY. National Bureau of Standards Circular 481. Pp. 14 + 11. U.S. Government Printing Office, Washington 25, D.C., U.S.A. Price 20 cents. plus 1/3rd postage.

#### **The Influence of a Single Echo on the Audibility of Speech**

By H. HAAS. Translated from German. Building Research Station, Department of Scientific and Industrial Research, Library Communication No. 303. Obtainable free by interested organizations and firms on written application to The Director, Building Research Station, Garston, Watford, Herts.

#### **B.B.C. Television Service : A Technical Description**

Pp. 32. British Broadcasting Corporation, The Grammar School, Scarle Road, Wembley, Middlesex. Price 2s.

#### **A Home Built Frequency Modulated Receiver**

By K. R. STURLEY, Ph.D., M.I.E.E. Pp. 85. *Electronic Engineering*, 28 Essex Street, Strand, London, W.C.2. Price 4s. 6d.

#### **Wireless at Sea**

By H. E. HANCOCK. Pp. 233 + xxxiii. Marconi International Marine Communication Co. Ltd., Chelmsford. Price 15s.

## **17TH NATIONAL RADIO EXHIBITION**

This exhibition is being held on 6th-16th September at Birmingham and elaborate plans are being made for the demonstration of television receivers in operation. There will be a viewing hall where the different exhibits will be working side by side and, in addition, demonstrations will be made on the individual stands.

A studio will be provided in the exhibition, and will be open to inspection by the public and a film scanner will also be available. These two sources of programme will provide demonstration material outside the normal transmission hours of Sutton Coldfield. The programme from this station will, of course, be used when it is suitable.

The sound and vision signals will be ' piped ' around the exhibition on carrier frequencies of 41.5 Mc/s and 45 Mc/s—the London frequencies. As a result all the receivers demonstrated will be London models. This is being done because it is impracticable to employ a local studio while Sutton Coldfield is operating if the distribution frequencies are the same as those of this station.

Some interference was experienced at the last London exhibition, although conditions there were less severe, and it is intended in future London exhibitions to adopt different carrier frequencies for distribution.

## **B.S.R.A. EXHIBITION**

An exhibition is being organized by the British Sound Recording Association and will be held at the Waldorf Hotel, Aldwych, London, on 20th and 21st May. There is space for twenty exhibitors and for demonstrations in a separate hall. Mobile recording equipment, provided by the B.B.C., E.M.I., Pathé Pictures and M.S.S. Recording, will be shown.

The exhibition will be open from 2.30 to 6.0 on the 20th and from 10.30 to 6.0 on the 21st and admission will be by catalogue, price 1s.

## **INSTITUTION OF ELECTRICAL ENGINEERS**

Meetings will be held at the I.E.E., Savoy Place, Victoria Embankment, London, W.C.2, on 18th May to commemorate the centenary of the birth of Oliver Heaviside. At 3 p.m. " Heaviside the Man " by Sir George Lee, O.B.E., M.C., followed at 5.30 by " An Appreciation of Heaviside's Contribution to Electromagnetic Theory " by Professor Willis Jackson, D.Sc., D.Phil.; " Heaviside's Operational Calculus " by Professor B. van der Pol, D.Sc.; " Fifty Years' Development in Telephone and Telegraph Transmission in Relation to the Work of Heaviside " by W. G. Radley, C.B.E., Ph.D. and " Some Unpublished Notes of Heaviside " by H. J. Josephs.

#### **Radio Section Meeting**

May 10th. " A Million-Volt Resonant-Cavity X-ray Tube," by B. Y. Mills, B.Sc., B.E. at 5.30 at I.E.E., London.

## **BRITISH INSTITUTE OF RADIO ENGINEERS**

**London Section.** May 25th at 6.30 at London School of Hygiene and Tropical Medicine, Keppel Street, W.C.1, " Multi Station V.H.F. Communication Systems Using Frequency Modulation," by E. G. Hamer and W. P. Cole, B.Sc.